


Article

The Impact of Sea Embankment Reclamation on Greenhouse Gas GHG Fluxes and Stocks in Invasive *Spartina alterniflora* and Native *Phragmites australis* Wetland Marshes of East China

Jian Li ^{1,2}, Zhanrui Leng ², Yueming Wu ², Guanlin Li ², Guangqian Ren ², Guirong Wu ³, Yongcan Jiang ⁴, Taitiya Kenneth Yuguda ^{2,*}  and Daolin Du ^{2,*}

¹ Key Laboratory of Original Agro-Environmental Pollution Prevention and Control/ Agro-Environment and Agro-Product Safety, Agro-Environment Protection Institution, Ministry of Agriculture and Rural Affairs, Tianjin 300191, China; Jianli@ujs.edu.cn

² Institute of Environment and Ecology, School of Environment and Safety Engineering, Jiangsu University, Zhenjiang 212013, China; 2212009001@stmail.ujs.edu.cn (Z.L.); wym@stmail.ujs.edu.cn (Y.W.); guanlinli1207@163.com (G.L.); rgq@ujs.edu.cn (G.R.)

³ College of Food and Biological Engineering, Hezhou University, Hezhou 542899, China; hzwgr510@163.com

⁴ PowerChina Huadong Engineering Corporation Ltd., Hangzhou 311122, China; jiang_yc4@hdec.com

* Correspondence: taitiyayuguda@ujs.edu.cn (T.K.Y.); ddl@ujs.edu.cn (D.D.)



Citation: Li, J.; Leng, Z.; Wu, Y.; Li, G.; Ren, G.; Wu, G.; Jiang, Y.; Yuguda, T.K.; Du, D. The Impact of Sea Embankment Reclamation on Greenhouse Gas GHG Fluxes and Stocks in Invasive *Spartina alterniflora* and Native *Phragmites australis* Wetland Marshes of East China. *Sustainability* **2021**, *13*, 12740. <https://doi.org/10.3390/su132212740>

Academic Editor: Vilém Pechanec

Received: 9 October 2021

Accepted: 12 November 2021

Published: 18 November 2021

Publisher's Note: MDPI stays neutral with regard to jurisdictional claims in published maps and institutional affiliations.



Copyright: © 2021 by the authors. Licensee MDPI, Basel, Switzerland. This article is an open access article distributed under the terms and conditions of the Creative Commons Attribution (CC BY) license (<https://creativecommons.org/licenses/by/4.0/>).

Abstract: The introduction of embankment seawalls to limit the expansion of the exotic *C₄* perennial grass *Spartina alterniflora* Loisel in eastern China's coastal wetlands has more than doubled in the past decades. Previous research focused on the impact of sea embankment reclamation on the soil organic carbon (C) and nitrogen (N) stocks in salt marshes, whereas no study attempted to assess the impact of sea embankment reclamation on greenhouse gas (GHG) fluxes in such marshes. Here we examined the impact of sea embankment reclamation on GHG stocks and fluxes of an invasive *Spartina alterniflora* and native *Phragmites australis* dominated salt marsh in the Dongtai wetlands of China's Jiangsu province. Sea embankment reclamation significantly decreased soil total organic C by 54.0% and total organic N by 73.2%, decreasing plant biomass, soil moisture, and soil salinity in both plants' marsh. It increased CO₂ emissions by 38.2% and 13.5%, and reduced CH₄ emissions by 34.5% and 37.1%, respectively, in the *Spartina alterniflora* and *Phragmites australis* marshes. The coastal embankment wall also significantly increased N₂O emission by 48.9% in the *Phragmites australis* salt marsh and reduced emissions by 17.2% in the *Spartina alterniflora* marsh. The fluxes of methane CH₄ and carbon dioxide CO₂ were similar in both restored and unrestored sections, whereas the fluxes of nitrous oxide N₂O were substantially different owing to increased nitrate as a result of N-loading. Our findings show that sea embankment reclamation significantly alters coastal marsh potential to sequester C and N, particularly in native *Phragmites australis* salt marshes. As a result, sea embankment reclamation essentially weakens native and invasive saltmarshes' C and N sinks, potentially depleting C and N sinks in coastal China's wetlands. Stakeholders and policymakers can utilize this scientific evidence to strike a balance between seawall reclamation and invasive plant expansion in coastal wetlands.

Keywords: coastal wetlands; wetland reclamation; seawalls; invasive species; salt marsh; alien plant invasion; climate change

1. Introduction

Global climate warming due to increased greenhouse gas (GHG) emissions from human activities is one of the most urgent challenges in ecology and climate change study [1]. Two of the most severe threats to world biodiversity are habitat alteration and the introduction and establishment of invasive species, especially in wetlands. Natural wetlands have been lost at a rate of 54–57% since pre-historic times, although it might have been as high as

87%. Wetland loss has accelerated (3.7 times) in the 20th and early 21st centuries due to continuing large-scale reclamation activities, with 64–71% of wetlands lost since the 1900s [2]. The introduction of coastal defenses and invasive species, which are developing at an increasing rate, are examples of human alterations of coastal environments [3]. These artificial structures combined with invasive species are now widely acknowledged as having synergistic negative impacts on the environment. Loss of coastal wetlands has prompted China to embark on more intensive coastline reclamation operations in recent decades [4]. Presently, thousands of kilometers of seawalls surround China's coastal wetlands, covering 60% of the whole length of mainland China's coastline [5]. The establishment of a vast number of seawall embankments has resulted in a significant loss of biodiversity and related ecosystem services in coastal wetlands [5–8]. Coastal wetlands are permanently or temporarily embanked in some restoration projects in China. They are sometimes entirely embanked and restored for agricultural or development reasons [9].

Coastal wetlands, despite accounting for only 6% of the earth's land surface, are essential carbon (C) sequesters as well as large GHG stocks and pools [10]. In addition, coastal embankments have been deployed to significantly reduce the spread of invasive species such as *Spartina alterniflora* (Yang et al., 2017a). However, significant land-cover alteration is linked to coastal embankments [11–14] and plant invasions [15–20] in past decades, with the impact on GHG emissions still to be fully assessed. The carbon footprint of a coastal engineering project is usually more significant and complicated than expected. The majority of marine projects involving quarried stone and concrete, such as dikes, seawalls, cofferdams, and other structures, are linked to CO₂ emissions during construction and operation [21]. Furthermore, it has been shown that reclamation of coastal wetlands alters the physicochemical features of coastal soils [22], affecting the sequestration capability and stability of the soil organic carbon pool [23].

The three GHGs—CO₂, N₂O, and CH₄—were influenced by the temperature of the sediment and the amount of plant biomass. Furthermore, CH₄ fluxes were associated with salinity, whereas N₂O fluxes were associated with photosynthetically active radiation. CO₂ fluxes fluctuated seasonally, as anticipated. Findings confirm that salt marshes with minimal nitrogen impacts do not contribute significant amounts of N₂O to the atmosphere [24]. CO₂ capture and eventual carbon sequestration may be influenced significantly by the wetlands' management and restoration history. As such, wetlands are frequently operating as a source of CO₂ while also increasing soil carbon deposition [25–27]. In China, for instance, continuous and significant wetland degradation and conversion amount to annual CO₂ emissions of approximately 6.83 Tg CO₂/yr [28]. *S. alterniflora*, an invasive species, and the increasing abundance of *P. australis*, a native plant, significantly elevated CH₄ emissions from marshes [29], whereas in other cases, plant species composition played an insignificant role in emitting CH₄ [30–32] and a crucial role in sequestering N₂O [32,33]. Carbon fluxes were highly associated with CH₄ fluxes in estuarine, freshwater marshes, where the major environmental drivers of CH₄ flux to the atmosphere are water temperature and wind speed [34]. Soil organic carbon (SOC) and mineral N, in contrast to CH₄, are key drivers affecting GHG flux from coastal and estuarine wetlands, which are extremely vulnerable to flooding from sea-level rise [35].

The importance of wetlands as carbon sinks varies greatly according to the hydrogeomorphology of the wetland and its location in the ecosystem. For instance, inorganic carbon content of sediment in mudflats was much lower than in vegetated habitats [36]. Further, although wetland habitats sequester carbon in their soil, the net balance of their C fluxes determines their real C sink potential. Several freshwater wetlands' potential to act as a net carbon sink is hampered by CH₄ emissions in particular [37]. Carbon and nitrogen dynamics significantly alter SOC dynamics following invasion by *S. alterniflora*, potentially altering C physical distribution in soil organic matter (SOM), essentially exhibiting a greater effect on SOC incorporation to facilitate SOC storage than soil organic nitrogen (SON) accumulation [38,39]. CO₂ sequestration linked with SOC burial generated by the invasive *S. alterniflora* would be largely offset by soil inorganic carbon SIC loss [40],

whereas tidal inundation enhances the net capture of CO₂ in a *Phragmites* salt marsh [41]. Plant invasions may alter the size and quality of the SOC pool, posing a threat to ecosystem function and the global carbon cycle [42]. Therefore, the time scale must be considered in assessing the relative constancy of C and N storage in coastal wetland soils [43]. Coastal wetlands and boreal peatlands are substantial C sinks (tons C/ha) according to global estimates of wetland pools. However, the lack of worldwide estimates per wetland type renders comparison to global C pool projections of saltmarshes, peatlands, and mangroves arduous [44]. The seemingly contradictory findings on GHG source-sink dynamics among coastal wetland ecosystems due to site-specific environmental circumstances [45] makes the quantification of the magnitudes and dynamics of coastal wetland GHG fluxes/stocks at regional and/or global scales essential [45,46].

Invasive alien plant species and coastal embankments have been studied in relation to the ecosystem dynamics of GHG fluxes and stocks in coastal wetlands. The diversity of plant species has a direct impact on GHG flux, as demonstrated by China's coastal wetlands, which pose a significant threat to global change [47]. The average CO₂, CH₄, and N₂O fluxes (ecosystem respiration) through coastal wetlands of China are determined to be $388.76 \pm 42.28 \text{ mg m}^{-2} \text{ h}^{-1}$, $2.20 \pm 0.31 \text{ mg m}^{-2} \text{ h}^{-1}$, and $16.44 \pm 2.96 \text{ mg m}^{-2} \text{ h}^{-1}$, respectively [47]. Contrary to other reports, the restored wetlands were found to be sources of CO₂ release rather than sinks [25,27]. In a *Typha* plant-dominated mesocosm, CH₄ releases were linked considerably with soil carbon, nitrogen, and surface biomass, increasing methane emissions up to three times $45.9 \pm 16.7 \text{ mg CH}_4\text{-C m}^{-2} \text{ h}^{-1}$ under high water elevations (Lawrence et al., 2017 [48]), whereas in an estuarine wetland in Ohio, USA, it was $219.4 \text{ g m}^{-2} \text{ yr}^{-1}$ (Rey-Sanchez et al., 2018 [34]). These were significantly higher than average yearly 18.7, 3.26, and $5.26 \text{ g m}^{-2} \text{ yr}^{-1}$ CH₄ flow from *S. alterniflora*, *P. australis*, and *C. malaccensis* predominant flora in a tropical coastal estuarine wetland in China, suggesting that *S. alterniflora*'s upper stalk, increasing CH₄ output, and extra efficient plant CH₄ delivery all contribute to the plant's higher CH₄ emission (Tong et al., 2012 [29]). *Spartina* soil had annual average CH₄ and N₂O fluxes of 13.77 and $1.14 \text{ mol m}^{-2} \text{ h}^{-1}$, respectively, which exceeds those of *Kandelia*, *Sonneratia*, and *Cyperus*, suggesting that the invasion of exotic wetland plants could transform coastal soils into a significant source of greenhouse gases while also increasing soil carbon deposition (Chen et al., 2015 [26]). Given the fact that CH₄ fluxes from mangrove, salt marsh, and seagrass environments vary greatly, they all function as net methane emitters., ranging from 67.33 to $72,867.83 \text{ mol CH}_4 \text{ m}^{-2} \text{ day}^{-1}$ for mangrove; 92.60 to $94,129.68 \text{ mol CH}_4 \text{ m}^{-2} \text{ day}^{-1}$ for marshland; and 1.25 – $401.50 \text{ mol CH}_4 \text{ m}^{-2} \text{ day}^{-1}$ for seagrass [49]. Total soil N₂O emissions from *S. alterniflora* communities in China are estimated to be approximately $0.06 \text{ Tg N}_2\text{O y}^{-1}$, accounting for about 0.60% of total N₂O emissions (9.6 – $10.8 \text{ Tg N}_2\text{O y}^{-1}$) (Gao et al., 2019 [50]).

Vast sea embankments have been built in *S. alterniflora* marsh to prevent its expansion and restore native *P. australis* marshes, which sea embankments have also confined as they grow inland [9]. Seawall-reclaimed wetland areas in the Yangtze River estuary increased by an average of $24,000 \text{ ha yr}^{-1}$, resulting in GHG flux rates of CO₂ and CH₄ that were 83.7×10^3 – $164 \times 10^3 \text{ mg m}^{-2} \text{ yr}^{-1}$ and 268 – $81.20 \times 10^3 \text{ mg m}^{-2} \text{ yr}^{-1}$, respectively [51]. Sea embankment reclamation significantly altered SOC and TN contents by 0.062% and 1.46%, respectively, compared to the values in the natural wetland of 0.053% and 1.30% (Zhou and Bi 2020 [52]); they decreased soil total organic C (233 to 495 g m^{-2}) by 50.60% and total organic N (22 to 46 g m^{-2}) by 49.99% (Yang et al., 2016 [53]), and they reduced soil TOC by 57% and TON by 59% in *S. alterniflora* salt marsh (Yang et al., 2017 [38]). A constructed seawall along the Coastal Line of Lake Nakaumi, Japan, influenced greenhouse gas emissions, with a high efflux of $245 \text{ mg CH}_4 \text{ m}^{-2} \text{ h}^{-1}$ during the day and $725 \text{ mg CO}_2 \text{ m}^{-2} \text{ h}^{-1}$ during the night (Hirota et al., 2007 [54]). According to a worldwide meta-analysis using a database of 209 sites to assess the impact of reclamation and land use cover changes of diverse wetland types, natural wetlands were found to be net sinks of atmospheric CO₂ and net sources of CH₄ and N₂O [55].

Reclamation by coastal embankments may alter GHG dynamics, according to our hypothesis, thus affecting plant development and soil physiochemical characteristics in invasive *S. alterniflora* and native *P. australis* salt marshes. The aim of this research was to evaluate the following hypothesis and questions: (1) The construction of a sea embankment in local habitats will dramatically increase greenhouse gas fluxes between the soil and the atmosphere in invasive *S. alterniflora* and native *P. australis* marshes; (2) whether soil carbon stocks vary between *S. alterniflora* and *P. australis* marshes in their response to sea embankment reclamation; and (3) whether there are differences in GHG fluxes and stocks between seawall restored *S. alterniflora* and *P. australis* marshes and adjoining unrestored *S. alterniflora* and *P. australis* marshes.

2. Materials and Methods

2.1. Study Area

The research site is in Dongtai, Jiangsu Province, China, and is close to China's Yellow Sea Coast (Figures 1 and 2). With a shoreline of 95 km, Dongtai is situated at 32°37'–33°0' N. This is a transitional zone with a monsoon climate and an average yearly temperature of 15 °C, mean temperature range −0.3–1.3 °C, with the lowest temperature of −17.3 °C. The average sunshine hours are 2199–2362 h, with solar radiation of 116.2×4.184 – 121.0×4.184 kJ cm^{−2} on average. The mean temperature range in July is 26.7–27.4 °C, with the highest temperature reaching 39 °C. The annual rainfall range is 980–1070 mm, with a mean annual rainfall of 1061 mm, with May and July accounting for about 70% of the total. Typhoons, rainstorms, hail, tornadoes, cold waves, and fog are just a few examples of extreme weather. The underwater intertidal period lasts 7–12 h. The tidal surge is approximately 1.27–4.61 m. The salinity is 2.953–3.224‰, with a pH of approximately 8 [56]. Mudflats in the low tide zone and salt marshes in the middle and high tidal zones make up Dongtai's estuary wetlands [57]. The offshore sediments of Dongtai are the largest in China and Jiangsu's most extensive land reserve. Their land area grew from 1268 km² in 1992 to 1300 km² in 1977. They enclose a sea body that is more than 200 km long (N–S) and 90 km wide (E–W). Even though actual evaluation planting on the offshore dunes failed, the 1996 breakthrough in seed dispersal and germination led to spontaneous spread throughout the 1 km wide coastal channel and was considered promising [58].

Since its introduction, the total area of *S. alterniflora* spread has increased dramatically. The plot, which was originally 3 km from the Dongtai–Dafeng border, had expanded into Dafeng tideland by 1992. *S. alterniflora* marsh with elevations ranging from 3.5 to 1.8 m has advanced about 1 km seaward, based on the 1.8 m elevation as the seaward marsh border. Its lush growth was determined to be best at heights of 2.0–2.5 m. The marsh was 1.1 km wide and covered 70% of the area [58]. Due to increased elevation, its landward portion was eventually replaced by *Suaeda salsa*. To combat the risk of *Spartina alterniflora* invasion, the Dongtai coastal administration began in 2011 erecting a 6163 km long seawall out of a total length of 15,339 km (Figures 3 and 4). The study area's soils are made up of marine and alluvial deposit materials, consisting of silt, sand, clay, and gravel, as well as a significant amount of organic matter. Its soil and natural plants were in fair shape at the time of enclosing. *Phragmites australis*, *Suaeda salsa*, *Spartina alterniflora*, and *Imperata cylindrica* var. covered approximately 80% of the soil [58].

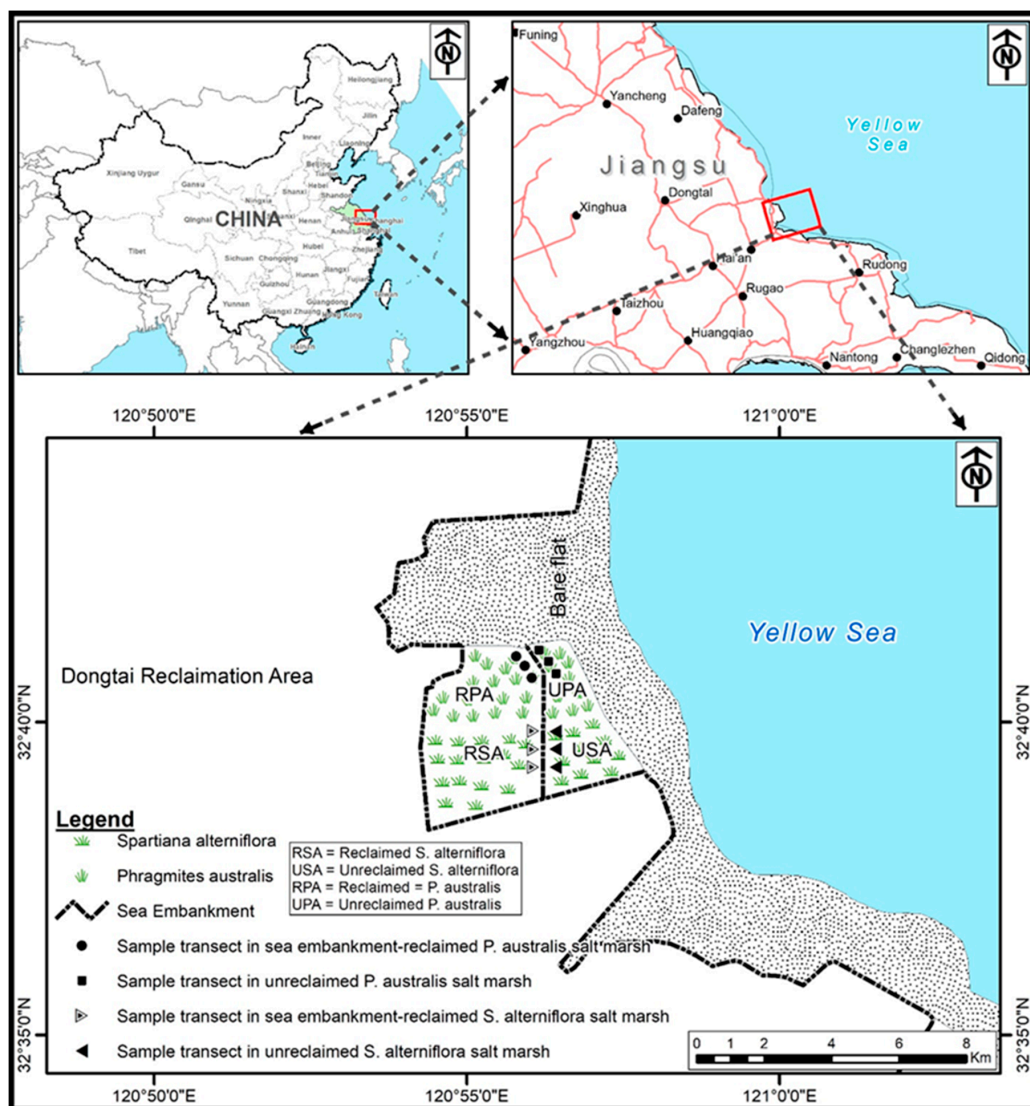


Figure 1. Location of the sampling site in Dongtai, Jiangsu, China.



Figure 2. Study area showing landscapes and vegetation.

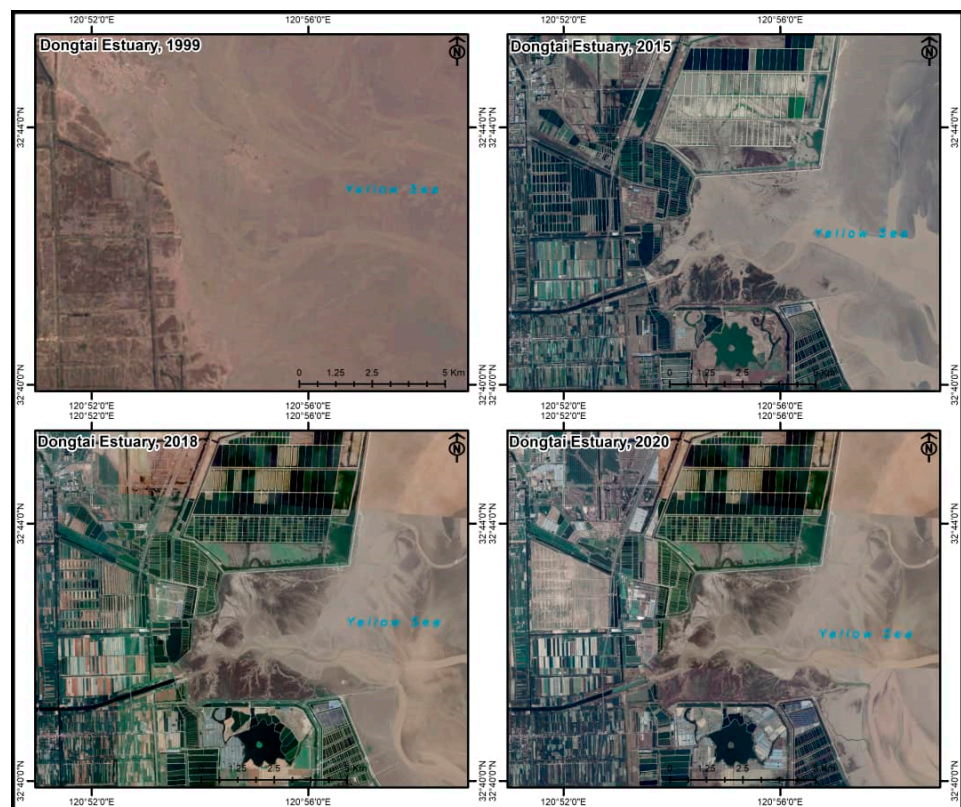


Figure 3. Land use and landcover changes due to *Spartina alterniflora* invasion and erection of reclamation seawalls.

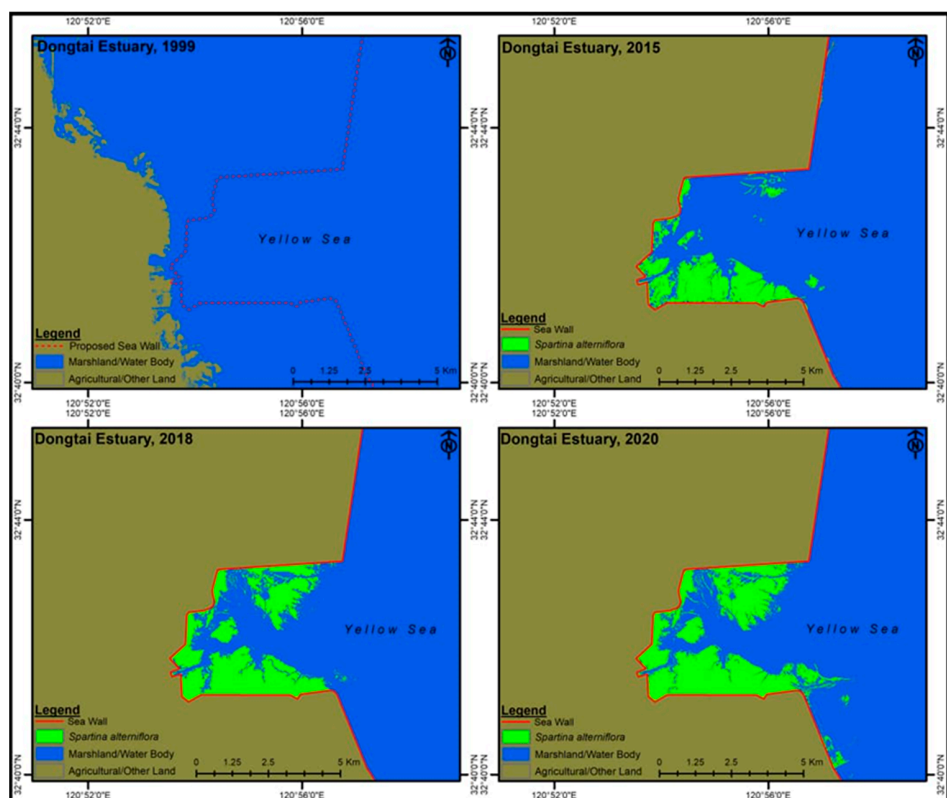


Figure 4. Study area showing *Spartina alterniflora* expansion before and after embankment reclamation.

2.2. Field Sample Collection

2.2.1. GHG Sampling and Flux Measurement

From January to September 2020, closed static chambers were used to monitor CO₂, CH₄, and N₂O fluxes eight different times to compare *P. australis* and *S. alterniflora* GHG emissions. Gas samples were taken from both sites simultaneously using the enclosed chamber method, and all sampling was completed 2 h before the least tidal cycle (G. C. Chen et al., 2010 [59]). Stainless steel collars of diameter 20 cm were driven 5 cm deep into the soil for at least 36 h before taking GHG readings. On the cylinder's side surface, a metal exhaust pipe of 1 mm diameter was installed (approximately 8 cm above the soil) to enable normalization of pressure disturbances between the chamber and surrounding environment. To produce a gas tight grip around the exhaust pipe, silicone adhesive was used. In January/February, three observations were taken on vegetated sediments and two observations taken on natively unvegetated sediments for both restored and unrestored marshes. Measurements were collected three times a month on both vegetated and unvegetated sediments in populations of both plant species from March to September. We assessed respiration without photosynthesis and saw changes in N₂O and CH₄ fluxes attributable to plant-catalyzed gas transfer by vegetation cover in unvegetated soils that were free of vegetation cover. Unvegetated soils were incidentally identical to vegetated strata and were as near as 1 m apart. Because the study marsh's plant density was low, we could insert gas flux flanges in between plants and take unvegetated observations within plant stands. With a diameter of 3 cm, the gas sampling port was located on top of the chamber. The hole was carefully covered with a plastic cork and closed with silicone glue once the chamber was lowered into the soil. Gas samples were obtained by piercing the plastic with the connected injectable needle into the chamber with a 10 mL glass syringe. An electric fan was installed in the chamber to ensure that the inside air was well mixed. We kept the air temperature within the chambers under control during the summer observations by enclosing the chamber top with cotton covers.

Gas samples of 25 mL were taken in duplicates immediately after securing the chamber for four more time periods, ranging from 30 to 60 min, by incorporating a 60 mL plastic syringe with a faucet through a plastic tube placed in the cylinder's side. The 25 mL gas samples were instantly introduced into the 12 mL Exetainer vials (Labco, CN) following the use of ultra-pure helium (UHP He) as a flush and then drained. To evaluate the soil-atmosphere fluxes of three greenhouse gases, we used the gas chromatography (GC) approach to assess concentrations of GHG within 30 days. Based on standards, the injector, column, and detector had temperatures of 100 °C, 70 °C, and 320 °C, accordingly sensitive to low levels of N₂O (Y. Chen et al., 2015 [26]). CH₄ and CO₂ concentrations were measured using the same GC system with a thermal conductivity detector (TCD). With nitrogen as the carrier gas, at a 20 mL min^{−1} flow rate, temperatures of 80 °C, 50 °C, and 80 °C were maintained for the injector, column, and detector, respectively (G. C. Chen et al., 2011 [60]). By correlating the peak area of gas samples to that of standard curves, the concentration of greenhouse gases was calculated. CO₂, CH₄, and N₂O had relative standard deviations of 2.8%, 2.7%, and 2.4%, respectively, in replicate standard measurements (Y. Chen et al., 2015 [26]). Each greenhouse gas's soil-atmosphere flux (F, mol m^{−2} h^{−1}) was calculated using the following formula (Chen et al., 2015) [26], Chen et al., 2016 [61]):

$$F = \frac{V \Delta G_c}{A \rho} \quad (1)$$

where V (m³) is the volume of air remaining inside the closed chamber after lowering the open end into the soil; ΔG_c (h^{−1}) is the variation in gas concentration inside the chamber; A (m²) is the surface area of soil enclosed by the chamber; and ρ (m³ mol^{−1}) is the volume of gas at air pressure.

N_2O and CH_4 GHG (CO_2 -eq) fluxes (Fe , $\text{mg CO}_2 \text{ m}^{-2} \text{ h}^{-1}$) were calculated using the following formula (Chen et al., 2015 [26]):

$$F_{\text{eq}} = F_{\text{GHG}} \times M_{\text{GHG}} \times \text{GWP}_{(\text{GHG})} \quad (2)$$

where F_{GHG} is the greenhouse gas flux, M_{GHG} is the greenhouse gas molecular weight, and $\text{GWP}_{(\text{GHG})}$ is the GHG global warming potential (with global warming potential of 23 and 296 CH_4 for and N_2O , respectively, on a time horizon of 100 years) (IPCC 2014 [62]).

2.2.2. Biomass and Soil Sampling

Following the completion of gas sampling, biomass and soil sampling were conducted. Three 50 cm by 50 cm quadrats were established in each transect of the coastline with restored and unrestored *S. alterniflora* and *P. australis* marshes to collect plant leaves, stems, and litter, and three soil segments (10 cm length by 10 cm breadth by 60 cm depth) were unearthed to extract roots. Four 40 m by 40 m transects were deployed in October 2020 in the seawall restored *S. alterniflora* marsh (RSA), *P. australis* salt marsh (RPA), unrestored *S. alterniflora* salt marsh (USA), and *P. australis* salt marsh (UPA) (Figure 1). According to assessments of Thematic Mapper satellite photos, the restored and unrestored *S. alterniflora* salt marshes in the survey area infringed on mudflats for a significant number of years (Chung et al., 2004 [58]). The density and height of the plants were measured on-site. Separate samples of aboveground biomass (AGB), belowground biomass (BGB), and litterfall biomass (LB) were taken. The AGB included the overall weight of leaves, branches, and stems. The sections for the BGB quantification were 1 m \times 1 m in size, with the depth of each section varying depending on the rooting depth. *Phragmites australis* roots are mainly found at ≥ 60 cm depth, and that of other species shallower in depth (Lu et al., 2019 [36]). The soil in each plot was scooped and gently cleaned through a fine screen to gather all the roots. The entire litter weight within the plot was included in the LB. Employing a balance (BSA124S-CW Sartorius), the fresh weight of the AGB, BGB, and LB parts from each quadrat were measured independently. For further analysis, each component was sub-sampled to roughly 100 g fresh weight. To establish a consistent weight, samples were oven-dried for at least 72 h at 60 °C, and their dry weight quantified to ascertain the water content. Each transect was divided into three 2 m by 2 m plots, with three spots chosen at random for sampling soil at depths of 0–10 cm, 10–20 cm, and 20–30 cm within every plot, and all soil samples were well mixed to obtain a blend for each section.

2.3. Laboratory Analyses

After filtering each soil sample through a 100-mesh sieve and properly flushing with water, the residual roots were amassed. For biomass measurement, a total of nine 1 m by 1 m plots were randomly chosen and garnered for each of the two main species. Fresh samples were properly cleaned and oven-dried for at least 72 h at 60 °C to quantify leaf, stem, litter, root, and total biomass. Forceps were used to extract organic materials from soil samples, which were then sieved at 2 mm and oven-dried to a consistent weight at 50 °C to evaluate the soil water content. The dry weight of the total sample span was divided by the volume of the core section to determine bulk density for each sample. An elemental analyzer (elementar UNICUBE) was used to determine the carbon and nitrogen content. Based on the above-measured carbon, nitrogen, and biomass values, the carbon pool of each portion was determined. A glass membrane electrode was used to determine soil pH in combination with a 1:2.5 soil-to-water ratio. A conductivity meter was used to determine the soil salinity combined with a 1:5 soil-to-water ratio (W. Yang, Li, et al., 2016 [9]).

2.4. Data Analysis

Stocks of organic and inorganic carbon in the sediments were examined following a prior evaluation [63]. The accrued carbon stocks in all layers were used to calculate the pools of inorganic and organic carbon (Mg C ha^{-1}) in 1 m soil strata, and the carbon pool in each stratum was calculated as the product of carbon metadata (% dry weight) and dry bulk density ($\text{g dry soil mL}^{-1}$). To calculate the quantity of CO_2 net sequestered, estimates of both the soil inorganic and organic carbon stocks were utilized. In soil formation, the net total CO_2 flux from the air to the soil can be computed using the following formula (Lu et al., 2019 [36]):

$$\text{CO}_{2\text{netseq}} = \text{CO}_C - \Psi C_{IC} \quad (3)$$

where CO_C is the organic carbon density in the sediment ($\text{mol C mL soil}^{-1}$); C_{IC} is the inorganic carbon density in the sediment ($\text{mol C mL soil}^{-1}$); Ψ is the predicted CO_2 and CaCO_3 gas exchange reaction ratio; and $\text{CO}_{2\text{netseq}}$ refer to the moles of CO_2 net sequestered in mL of soil. The value of $\Psi = 0.6$ for shallow coastal sites was used in this estimation [64,65]. All data were reported as the average of three replicates' averages and standard deviations. Prior to testing with analysis of variance (ANOVA), the data for each variable were examined for homogeneity and then log-transformed if necessary. Using ANOVA and Tukey HSD multiple comparisons, the differences in plant characteristics and carbon content of the AGB, BGB, and LB between the two plant marshes were investigated. The carbon fluxes and pools (AGB, BGB, and LB) were then estimated using the biomass and carbon content data. SPSS version 16.0 was used for all statistical analyses (SPSS Inc., Chicago, IL, USA). Obtained carbon storage and flux data were then compared to the carbon fluxes and stocks published in Web of Science relevant papers.

3. Results

3.1. Plant Biological Characteristics and Biomass Carbon Pool

S. alterniflora was taller ($F = 22.6$, $p = 0.001$) and had a higher plant density ($F = 12.5$, $p < 0.001$) than *P. australis*. Plant root (0–60 cm soil depth) and stem biomass were considerably lower in the restored *P. australis* salt marsh compared to the unrestored *P. australis* salt marsh, whereas AGB and total biomass were significantly lower in the restored *S. alterniflora* salt marsh than in the unrestored *S. alterniflora* salt marsh (Figure 5a,b). Conversely, litter biomass was much higher in the restored *P. australis* salt marsh compared to the unrestored. However, there were no statistically significant variations in leaf biomass and total biomass between the unrestored and restored *P. australis* salt marshes (Figure 5b). Overall, the unrestored *S. alterniflora* marsh had the most AGB, BGB, and LB. Both AGB and LB carbon content were identical for both plants (both $p < 0.001$), whereas the BGB carbon content was significantly higher for UPA ($31.16 \pm 0.8\%$) and RPA ($29.34 \pm 0.8\%$) than for USA ($9.94 \pm 1.7\%$) or RSA ($7.46 \pm 1.8\%$). This suggests that *P. australis* roots play a significant role in carbon sequestration, regardless of the presence of the sea embankment. Overall, the highest AGB carbon content was found in unrestored *S. alterniflora*, the highest BGB carbon content was found in unrestored *P. australis*, and the highest LB carbon content was found in unrestored *S. alterniflora* ($p < 0.001$). The data show that the sea embankment affects the carbon sequestration potential of both *P. australis* and *S. alterniflora* plants, notwithstanding the slight variations in the restored and unrestored biomass carbon content marshes.

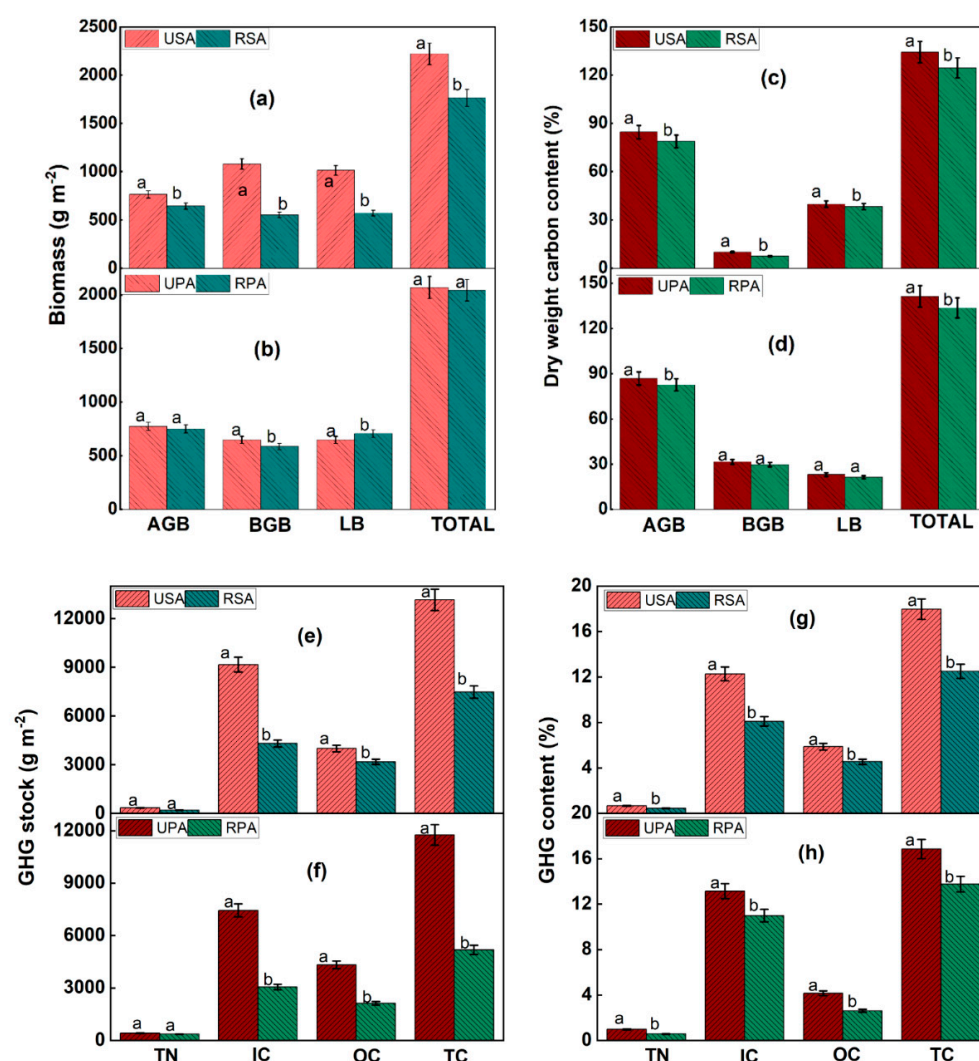


Figure 5. (a,b) plant biomass, (c,d) biomass dry weight carbon content, (e,f) biomass GHG stock and (g,h) biomass GHG content in each month. Error bars indicate mean \pm standard error ($n = 3$). USA = unrestored *S. alterniflora* salt marsh; RSA = sea embankment-restored *S. alterniflora* salt marsh; UPA = unrestored *P. australis* salt marsh; RPA = sea embankment-restored *P. australis* salt marsh.

3.2. Soil Carbon C and Nitrogen N Pools

Both water content and bulk density showed substantial correlations between habitats and core depths. The *P. australis* habitats had much lower mean water content than the *S. alterniflora* marsh. In both restored and unrestored marshes, water content increased steadily with increasing core depth (Table 1), whereas bulk density increased significantly with core depth for the first 40 cm in all marshes. Reclamation by sea embankments had a significant impact on SOC, SIC, and total N (Table 2). SOC, SIC, and total N concentrations were positively correlated across species in unrestored and restored salt marshes, and all had significant positive correlations with soil moisture and salinity (Table 3). Nonetheless, there were substantial negative linkages observed between varying organic carbon and nitrogen components in the soil, as well as soil bulk density and pH (Table 3). Accumulation of SOC, SIC, and total N were much lower in the restored *S. alterniflora* salt marsh than in the unrestored. In the unrestored and restored *S. alterniflora* salt marshes, the SOC stock varied from 397 to 994 g m⁻² and 398 to 633 g m⁻², respectively, whereas in the *P. australis* marshes, it varied from 438 to 831 g m⁻² and 247 to 496 g m⁻², respectively (Figure 5e,f). In the *S. alterniflora* marsh, SIC stock varied from 1108 to 1786 g m⁻² USA and 485 to 914 g m⁻² RSA, respectively, whereas in the *P. australis* marshes it varied from 1007 to

1650 g m⁻² UPA and 309 to 622 g m⁻² RPA, respectively. Nitrogen N content varied from 33 to 91 g m⁻² in the USA, 24 to 59 g m⁻² in the RSA, whereas for *P. australis*, it varied from 45 to 88 g m⁻² UPA and 36 to 74 g m⁻² RPA, respectively (Figure 5e,f). In the restored *S. alterniflora* salt marsh, SOC, SIC, and N stocks in the 0–60 cm depth declined by 20.5%, 52.9%, and 41.2%, respectively, compared to the unrestored marsh (Figure 5g,h), whereas it declined by 50.8%, 58.9%, and 11.4%, respectively, in the *P. australis* marshes.

With the exception of SOC in the *S. alterniflora* 20–60 cm depth and N stocks in the *P. australis* 20–40 cm soil-depth range, significant variations in soil (0–60 cm depth) SIC and TC stocks were identified in both the unrestored and restored salt marshes of both plants. Significantly low TOC ratios in the USA and RSA marshes and low TN ratios in the UPA and RPA marshes show that the SOC content of the *S. alterniflora* salt marsh and the N content of the *P. australis* wetlands were not significantly influenced by reclamation seawalls. Overall, our findings revealed that habitat and core depth significantly impacted inorganic carbon, organic carbon, and total nitrogen (Table 1). For organic carbon and total nitrogen, there was a strong link between biome and core depth ($p < 0.05$), and the reverse was true for inorganic carbon content ($p > 0.05$).

Table 1. Soil physical properties and carbon and nitrogen content (mean \pm SE, $n = 54$) in the unreclaimed and seawall-reclaimed *S. alterniflora* and *P. australis* salt marshes. Lower-case superscript letters (^{a,b}) indicate statistical significance at $p < 0.05$ between the unreclaimed and sea embankment-reclaimed salt marshes in the same community and at the same soil depth.

	Depth (cm)	Moisture (%)	BD (g cm ⁻³)	Salinity (%)	pH	IC Content (%)	OC Content (%)	Total Carbon TC (%)	Nitrogen Content (%)	OC/TN
USA	0–10	62.96 \pm 1.36 ^b	0.88 \pm 0.04 ^a	1.65 \pm 0.05 ^a	8.44 \pm 0.05 ^a	1.55 \pm 0.13 ^a	1.21 \pm 0.10 ^b	2.76 \pm 0.25 ^a	0.27 \pm 0.02 ^b	4.50 \pm 0.08 ^a
	10–20	50.10 \pm 2.14 ^b	0.96 \pm 0.02 ^a	1.43 \pm 0.04 ^a	8.41 \pm 0.08 ^a	2.32 \pm 0.11 ^b	1.53 \pm 0.13 ^b	3.85 \pm 0.15 ^b	0.11 \pm 0.01 ^a	13.82 \pm 0.96 ^b
	20–30	43.7 \pm 1.14 ^a	1.00 \pm 0.05 ^b	1.51 \pm 0.05 ^a	8.40 \pm 0.04 ^a	2.12 \pm 0.10 ^b	0.87 \pm 0.10 ^a	2.99 \pm 0.10 ^a	0.09 \pm 0.01 ^a	9.60 \pm 1.95 ^b
	30–40	42.5 \pm 1.00 ^a	1.20 \pm 0.09 ^b	1.50 \pm 0.10 ^a	8.37 \pm 0.04 ^a	2.22 \pm 0.08 ^b	0.83 \pm 0.05 ^a	3.05 \pm 0.07 ^b	0.07 \pm 0.01 ^a	12.74 \pm 1.14 ^b
	40–50	42.1 \pm 0.68 ^a	1.21 \pm 0.06 ^b	1.53 \pm 0.06 ^a	8.22 \pm 0.05 ^a	1.97 \pm 0.04 ^a	0.66 \pm 0.05 ^a	2.63 \pm 0.13 ^a	0.07 \pm 0.01 ^a	10.88 \pm 2.41 ^b
	50–60	40.7 \pm 0.58 ^a	1.10 \pm 0.07 ^b	1.48 \pm 0.06 ^a	8.31 \pm 0.07 ^a	2.21 \pm 0.09 ^b	0.58 \pm 0.05 ^a	2.79 \pm 0.19 ^a	0.05 \pm 0.01 ^a	11.83 \pm 0.47 ^b
RSA	0–10	34.46 \pm 1.46 ^b	1.11 \pm 0.05 ^a	0.57 \pm 0.03 ^b	9.00 \pm 0.03 ^a	1.57 \pm 0.16 ^a	1.11 \pm 0.06 ^b	2.36 \pm 0.08 ^b	0.10 \pm 0.07 ^b	7.82 \pm 2.56 ^a
	10–20	27.89 \pm 1.05 ^a	1.29 \pm 0.10 ^a	0.42 \pm 0.03 ^b	9.12 \pm 0.03 ^a	1.34 \pm 0.08 ^a	0.79 \pm 0.06 ^a	2.45 \pm 0.10 ^b	0.09 \pm 0.01 ^b	12.22 \pm 2.01 ^b
	20–30	26.74 \pm 0.80 ^a	1.30 \pm 0.12 ^a	0.37 \pm 0.02 ^b	9.24 \pm 0.05 ^a	1.34 \pm 0.11 ^a	0.69 \pm 0.06 ^a	2.03 \pm 0.08 ^b	0.06 \pm 0.00 ^a	11.5 \pm 1.71 ^b
	30–40	26.31 \pm 1.02 ^a	1.32 \pm 0.09 ^a	0.35 \pm 0.03 ^b	9.27 \pm 0.04 ^a	1.29 \pm 0.03 ^a	0.67 \pm 0.05 ^a	1.96 \pm 0.10 ^a	0.05 \pm 0.00 ^a	14.83 \pm 0.72 ^b
	40–50	26.01 \pm 0.38 ^a	1.34 \pm 0.06 ^a	0.31 \pm 0.02 ^b	9.28 \pm 0.04 ^a	1.26 \pm 0.06 ^a	0.59 \pm 0.06 ^a	1.85 \pm 0.07 ^a	0.05 \pm 0.01 ^a	12.04 \pm 2.50 ^b
	50–60	24.88 \pm 0.65 ^a	1.32 \pm 0.04 ^a	0.40 \pm 0.04 ^b	9.31 \pm 0.03 ^a	1.30 \pm 0.04 ^a	0.61 \pm 0.02 ^a	1.91 \pm 0.04 ^a	0.03 \pm 0.00 ^a	18.92 \pm 1.10 ^b
UPA	0–10	21.8 \pm 1.14 ^a	0.8 \pm 0.08 ^a	0.95 \pm 0.08 ^a	8.67 \pm 0.07 ^a	2.00 \pm 0.18 ^a	1.02 \pm 0.15 ^b	3.02 \pm 0.17 ^b	0.12 \pm 0.01 ^a	8.64 \pm 2.41 ^b
	10–20	22.4 \pm 1.08 ^a	1.3 \pm 0.08 ^b	0.91 \pm 0.05 ^a	8.76 \pm 0.05 ^a	1.79 \pm 0.07 ^a	0.99 \pm 0.04 ^b	2.78 \pm 0.12 ^a	0.16 \pm 0.02 ^a	6.22 \pm 0.47 ^b
	20–30	22.1 \pm 0.93 ^a	1.7 \pm 0.10 ^b	0.81 \pm 0.05 ^a	8.80 \pm 0.07 ^a	2.91 \pm 0.08 ^b	0.50 \pm 0.04 ^a	3.41 \pm 0.16 ^b	0.21 \pm 0.02 ^b	2.55 \pm 0.39 ^a
	30–40	20.2 \pm 1.24 ^a	1.9 \pm 0.19 ^b	0.72 \pm 0.04 ^a	8.84 \pm 0.06 ^a	1.93 \pm 0.16 ^a	0.30 \pm 0.01 ^a	2.23 \pm 0.06 ^a	0.25 \pm 0.02 ^b	1.25 \pm 0.12 ^a
	40–50	22.7 \pm 0.77 ^a	1.8 \pm 0.06 ^b	0.70 \pm 0.04 ^a	8.88 \pm 0.04 ^a	2.05 \pm 0.06 ^a	0.51 \pm 0.11 ^a	2.56 \pm 0.17 ^a	0.13 \pm 0.01 ^a	4.12 \pm 1.31 ^b
	50–60	22.1 \pm 1.34 ^a	1.8 \pm 0.10 ^b	0.71 \pm 0.05 ^a	8.91 \pm 0.05 ^a	2.45 \pm 0.16 ^b	0.55 \pm 0.05 ^a	3.00 \pm 0.06 ^b	0.08 \pm 0.01 ^a	7.12 \pm 0.45 ^b
RPA	0–10	18.0 \pm 0.78 ^b	1.1 \pm 0.08 ^a	0.63 \pm 0.02 ^a	8.92 \pm 0.03 ^a	1.56 \pm 0.13 ^a	0.16 \pm 0.01 ^a	1.72 \pm 0.08 ^a	0.06 \pm 0.01 ^a	2.82 \pm 0.29 ^a
	10–20	12.8 \pm 1.25 ^a	1.3 \pm 0.09 ^a	0.59 \pm 0.02 ^a	8.99 \pm 0.03 ^a	1.87 \pm 0.12 ^a	0.17 \pm 0.01 ^a	2.04 \pm 0.08 ^b	0.08 \pm 0.01 ^a	2.22 \pm 0.06 ^a
	20–30	10.8 \pm 0.87 ^a	1.6 \pm 0.16 ^b	0.65 \pm 0.01 ^a	9.08 \pm 0.02 ^a	2.02 \pm 0.06 ^b	0.52 \pm 0.04 ^b	2.54 \pm 0.16 ^b	0.11 \pm 0.01 ^a	4.82 \pm 0.42 ^b
	30–40	10.1 \pm 0.43 ^a	1.8 \pm 0.08 ^b	0.55 \pm 0.01 ^a	9.03 \pm 0.03 ^a	1.07 \pm 0.02 ^a	0.92 \pm 0.04 ^b	1.99 \pm 0.11 ^a	0.15 \pm 0.01 ^b	6.23 \pm 0.39 ^b
	40–50	14.8 \pm 0.52 ^b	1.8 \pm 0.16 ^b	0.53 \pm 0.01 ^a	9.01 \pm 0.03 ^a	1.88 \pm 0.06 ^a	0.45 \pm 0.05 ^b	2.33 \pm 0.17 ^b	0.11 \pm 0.01 ^a	4.11 \pm 0.07 ^b
	50–60	17.3 \pm 1.32 ^b	2.1 \pm 0.09 ^b	0.50 \pm 0.02 ^a	8.89 \pm 0.02 ^a	2.67 \pm 0.10 ^b	0.34 \pm 0.01 ^b	3.01 \pm 0.08 ^b	0.06 \pm 0.01 ^a	5.69 \pm 0.39 ^b

Table 2. Statistical significance of the effects of community, reclamation, depth, and their interactions on soil C and N based on three-way ANOVA.

Variation Source	Nitrogen Content (g kg ⁻¹)	OC Content (g kg ⁻¹)	IC Content (g kg ⁻¹)	Total Carbon TC (g kg ⁻¹)
Community	95.735 ***	159.418 ***	258.261 ***	439.371 ***
Reclamation	106.372 ***	125.597 ***	196.151 ***	275.256 ***
Depth	54.264 ***	51.878 ***	65.841 ***	108.867 ***
Community × Reclamation	58.689 ***	68.245 ***	111.344 ***	179.327 ***
Community × Depth	5.449 *	9.505 ***	15.608 ***	37.598 ***
Reclamation × Depth	6.110 **	7.579 ***	9.905 **	14.356 ***
Community × Reclamation × Depth	0.870	0.254	2.421 *	12.413 ***

* $p < 0.05$, ** $p < 0.01$, *** $p < 0.001$.**Table 3.** Correlation analysis of litter and root biomass, soil physical and chemical properties, and soil C and N fractions across communities in the unreclaimed and embankment- reclaimed salt marshes.

	LB	RB	Moisture	BD	pH	Salinity	SOC	SIC	TN	TC
SOC	0.892 **	0.836 **	0.961 **	−0.837 **	−0.985 **	0.824 **	1			
SIC	0.879 **	0.974 **	0.796 **	−0.931 **	−0.987 **	0.831 **	0.79 **	1		
TN	0.829 **	0.889 **	0.849 **	−0.92 **	−0.894 **	0.787 **	0.784 **	0.881 **	1	
TC	0.891 **	0.846 **	0.873 **	−0.791 **	−0.897 **	0.843 **	0.949 **	0.953 **	0.873 *	1

* $p < 0.05$; ** $p < 0.01$; LB: litter biomass; RB: root biomass.

3.3. Greenhouse Gas (GHG) Fluxes

Both vegetation type and reclamation forms significantly impacted greenhouse gas fluxes between the soil and the atmosphere (Table 4). CO₂ fluxes for both species were similar, whereas there were differences between embankment restored and unrestored segments and over the span of the year. The atmospheric flux of all three GHGs was positively correlated with soil temperature, water content, biomass, TOC, TIC, and TN but negatively correlated with soil pH (Table 5). Slightly above a quarter (27%) of the fluxes recorded were nil or beyond observation limits. CO₂ fluxes were either zero or positive in January to May of both transect sections, at which photosynthesis is limited by composition, indicating net CO₂ release (Figure 6a,b).

Table 4. Outcomes of a two-way ANOVA on soil-plant-atmosphere fluxes of three greenhouse gases showing the interactions between vegetation type and reclamation type.

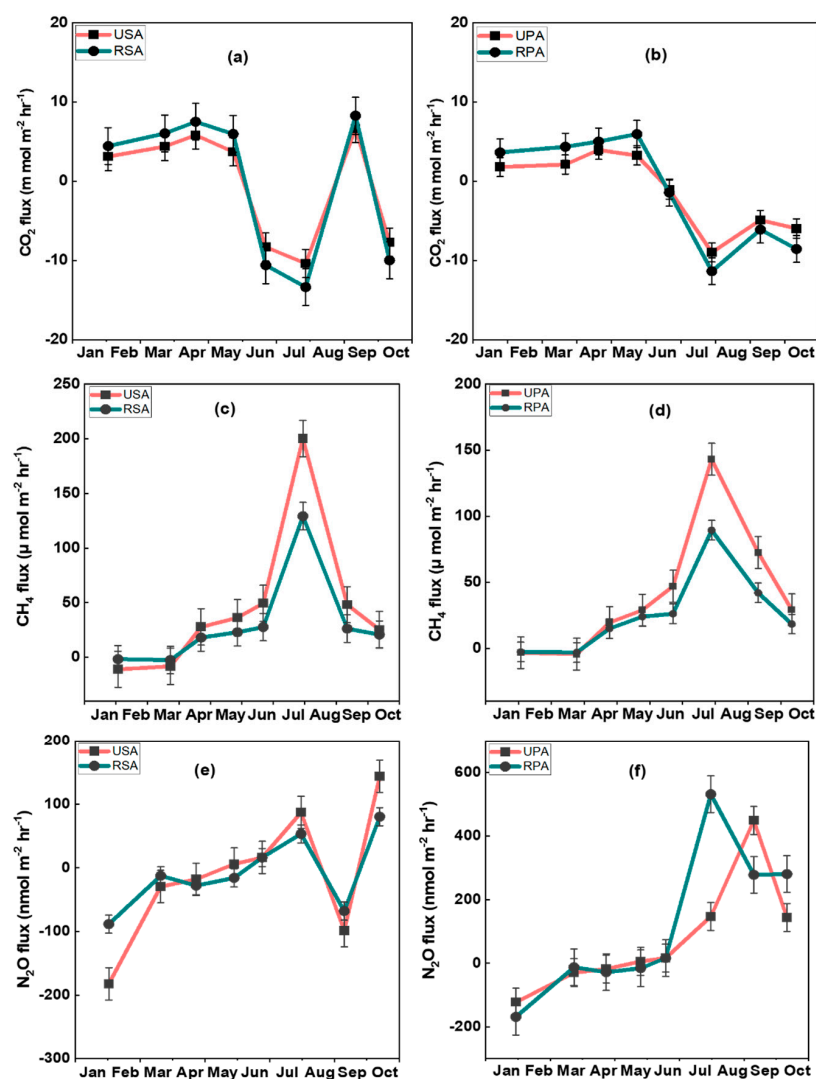
Greenhouse Gases	Variation Source	df	F-Value
CO ₂ (m mol m ⁻² h ⁻¹)	Vegetation type	2	6.13 **
	Reclamation type	2	3.13 ***
	Vegetation type × Reclamation type	4	0.053 ***
CH ₄ (μ mol m ⁻² h ⁻¹)	Vegetation type	2	0.11 ***
	Reclamation type	2	1.19 ***
	Vegetation type × Reclamation type	4	0.013 ***
N ₂ O (n mol m ⁻² h ⁻¹)	Vegetation type	2	3.49 ***
	Reclamation type	2	0.60 ***
	Vegetation type × Reclamation type	4	0.76 ***

** Significant difference which represents $p < 0.05$. *** Significant difference which represents $0.001 < p < 0.01$.

Table 5. The relationship between soil-plant characteristics and greenhouse gas fluxes employing Pearson correlation coefficients (r).

Soil Properties	Fluxes of Greenhouse Gases		
	CO ₂	CH ₄	N ₂ O
Water content	0.612 **	0.355 *	0.381 **
Soil temperature	0.777 *	0.411 **	0.608 *
AGB	0.833 *	0.422 **	0.107
BGB	0.747 **	0.269	0.864 **
PH	−0.008	−0.196	−0.279
Salinity	0.84 **	0.91 *	0.73 *
TOC	0.612 *	0.401	0.432
TIC	0.924 *	0.715	0.613
TN	0.162	0.415	0.034

* Represents significant difference at $0.01 < p < 0.05$. ** Represents significant difference at $0.001 < p < 0.01$.

**Figure 6.** Greenhouse fluxes in each month; (a,b) carbon dioxide fluxes, (c,d) methane fluxes (e,f) nitrous oxide fluxes Error bars indicate means \pm standard error ($n = 3$). USA = unrestored *S. alterniflora* salt marsh; RSA = sea embankment-restored *S. alterniflora* salt marsh; UPA = unrestored *P. australis* salt marsh; RPA = sea embankment-restored *P. australis* salt marsh.

In the months of January to May, CO₂ fluxes from embankment restored parts were also either zero or positive, identical to unrestored sections, but immediately AGB became significantly available for photosynthesis to counteract respiration rates, and CO₂ fluxes turned negative (Figure 6a,b). CO₂ fluxes from restored sections were much higher in April, July, and September than fluxes from the restored sections in June, July, and September. In July, CO₂ uptake in restored segments for both plants were significantly higher (13.98 m mol m⁻² h⁻¹ RSA and 11.34 m mol m⁻² h⁻¹ RPA) than in any other months. According to Pearson correlation analysis, the most critical determinants of CO₂ fluxes were live AGB and soil temperature, which combined accounted for over half of the variance in CO₂ flux data (Table 5).

CH₄ fluxes for both plants in embankment restored and unrestored sections were similar, although fluxes varied by season. Positive and negative CH₄ flux values indicated the occurrence of methanogenesis (Figure 6c,d). Except for July, where CH₄ fluxes reached 200 µ mol m⁻² h⁻¹, the bulk (90%) of CH₄ fluxes were between −10 and 50 µ mol m⁻² h⁻¹. In July, the CH₄ flux in the USA marsh (200.32 µ mol m⁻² h⁻¹) was more than all other reclamation types, with RSA having 129.23 µ mol m⁻² h⁻¹, UPA 143.19 µ mol m⁻² h⁻¹, and RPA 89.45 µ mol m⁻² h⁻¹, respectively. According to correlation analysis, the most relevant indicators of CH₄ flux obtained in this study were live AGB, sediment temperature, and salinity. Together, they account for approximately 40% of the fluctuation in CH₄ emissions (Table 5). In embankment restored marshes, N₂O fluxes ranged from −421 to +534.16 n mol m⁻² h⁻¹, whereas in unrestored marshes, fluxes ranged from −143.64 to 531.40 n mol m⁻² h⁻¹. Sixty-eight percent of all flux estimations, however, were nil or below observation limits. The mean flux was close to zero at 17 n mol m⁻² h⁻¹, whereas the median flux was 0. Although there were similar patterns in N₂O fluxes between both marshes, the RSA and RPA marshes showed significantly contrasting fluxes in the summer months. From July to September, N₂O fluxes in the RSA marsh varied significantly from −67.94 to 80.27 n mol m⁻² h⁻¹, whereas in the RPA marshes it varied from 16.21 to 531.40 n mol m⁻² h⁻¹ (Figure 6e,f). Although seasonal fluctuation is still evident, the importance of sediment temperature in the correlation analysis shows that other seasonal variations would be expected. Summer months showed a modest net positive emission rate of 105 ± 48 n mol m⁻² h⁻¹, whereas cooler months had a lower net absorption rate of −64 ± 47 n mol m⁻² h⁻¹ (mean ± standard error) in the unrestored marshes. The results of the correlation analysis indicate that sediment temperature and live BGB influence N₂O flux rate (Table 5). Overall, these indicators predicted about half of the variation in N₂O fluxes (49%).

4. Discussion

4.1. Spatial Variations and Determinants of Soil Carbon and Nitrogen Stocks

The robust relationships observed in both restored and natural wetlands between SOC and plant community cover, overall vegetation cover, BGB, soil C:N, and soil salinity support the theory that all have a significant impact on SOC [52,66,67]. Findings show that in the 0–60 cm soil depth of *S. alterniflora* salt marsh, sea embankment reclamation reduced SIC by 33.6% and total carbon TC by 30.5%, whereas in the *P. australis* marsh, reductions were 15.4% and 23.5%, respectively (Figure 5g,h). Decrease in dry weight carbon content was slightly significant, 25% in the BGB of the *S. alterniflora* marsh compared to the other biomass categories (Figure 5g,h). Plant-residuals input and SOM degradation are well-known factors influencing sequestration of soil organic carbon and nitrogen [9,52]. Preceding research found that embankment walls can limit *S. alterniflora* development and inhibit tidal flooding flows and salt marsh inundation caused by precipitation or irrigation. As such, *S. alterniflora* is hampered from completing its regular life cycle in freshwater habitats, whereas mild salinity promotes its growth by accelerating flowering [68,69]. Our study corroborates these findings, as shown in Table 1 and Figure 5a–d. In the *S. alterniflora* salt marsh, reclamation by seawalls greatly degraded soil salinity (0–60 cm depth) from 1.52% to 0.40%, LB from 1012 g m⁻² to 569.6 g m⁻², and root biomass from

1078 g m⁻² to 551.3 g m⁻². In comparison to native *P. australis*, *Scirpus mariqueter*, *S. salsa*, and *Cyperus* marshes of eastern China, *S. alterniflora* invasion often promotes soil organic carbon and nitrogen sequestration by enhancing LB and BGB feeds and decreasing SOM breakdown [9,26,69,70].

The lesser litter production and root biomass resulted in a considerable decline in soil SOC and TN in the embankment-restored marsh (Table 1). There are two possible explanations for these alterations. First, the recovered wetland had decreased production recovery and yield rates compared to native intertidal wetland because it is a relatively dry habitat [71]. Furthermore, because of the increased rate of organic carbon sequestration in wetland soils, native marsh can influence prolonged carbon capture [72]. Second, the restored *S. alterniflora* salt marsh diminished LB and BGB soil inputs, resulting in soil organic carbon and nitrogen stocks degradation (Figure 5e–h).

Additionally, because of the hypoxic soil conditions that support lengthy deposition of SOM, marshes with high water content or water tables are favorable for SOM accumulation [9,73]. Recurrent tidal flooding of salt marshes can be hampered by sea embankments, resulting in significant declines in soil water levels [23]. The soil moisture in the restored *S. alterniflora* salt marsh dropped dramatically, from 46.67% to 27.752% (Table 1), potentially increasing SOM breakdown and speeding up the deficiency of soil organic carbon and nitrogen. This could speed up the degradation of SOM and the loss of soil organic carbon and nitrogen [9]. The average SOC and TN were lower in the embankment-restored marsh transects than in the restored marsh (Table 1), which could elucidate why the seawall-restored marsh has more spatial variability of plant species. The mean values of soil SOC and TN may be affected by habitat degradation in an embankment-restored wetland. These findings also emphasized the necessity of characterizing regional patterns of soil characteristics and uneven vegetation.

4.2. Environmental Drivers of Greenhouse Gas (GHG) Fluxes

Although China's wetlands constitute a net carbon sink, they also release CO₂ and CH₄ from the soil, making them a substantial source of atmospheric carbon. However, the volume of emissions differed greatly depending on the type of wetland. The tropical location, expanse of mangrove vegetation, periodic shoreline flooding, and moderate weather are all factors that contribute to the highest carbon emissions in coastal wetlands. Higher elevations and latitudes decreased soil CO₂ and CH₄ emissions in marsh wetlands and may be responsible for the low annual temperature and a delayed growing season for grassland plants [74]. Furthermore, the shortage of aquatic plants and low CO₂ and CH₄ emissions in river and lake wetlands could be linked to their lengthy flooding regimes [75]. In addition to the impact of photosynthesis on fluxes of CO₂, we observed significant fluctuations in N₂O fluxes across the restored sections of the *S. alterniflora* and *P. australis* marshes (Figure 6e,f). Though unrestored sections had more live belowground biomass, the matching of biogeochemical properties was attributable to the plants' closeness to the unvegetated plots. Because the existence or absence of plants had no effect on observations, CH₄ or CO₂ fluxes were attributed to biomass characteristics. As a result, we infer that wetland plants influenced GHG emissions by modifying the soil instead of plant-induced diffusion [24]. Live AGB was negatively linked to fluxes of CO₂ (i.e., the higher the biomass, the more negative the flux) and strongly linked to soil temperature in the correlation analysis. Although live AGB was the most critical indicator of GHGs ($p < 0.001$), sediment temperature was another critical predictor, particularly in unrestored areas, according to correlation analysis.

The highest CO₂ emissions obtained (587.4 mg m⁻² h⁻¹) in the unrestored *S. alterniflora* marshes occurred in later summer month (Figure 6a), which coincided with the hottest weather and driest sediments (Table 4). This value far exceeds the average CO₂ emissions (388.76 ± 42.28 mg m⁻² h⁻¹) across coastal wetlands in China [47], indicating the seawall embankment played a significant role in carbon emissions. However, [24] observed that invasive *P. australis* marsh emits up to 660 mg m⁻² h⁻¹ CO₂, whereas the unvegetated

marsh could emit up to $880 \text{ mg m}^{-2} \text{ h}^{-1}$ of CO_2 . Thus, net CO_2 uptake in embankment restored areas was highest during the time of intense biomass production in June and July but fell significantly in August and September (Figure 6a,b). This occurrence is influenced by a peak in ecosystem respiration and delayed photosynthetic uptake senescence.

The considerable spatial-temporal changes in CH_4 flux were explained by a positive correlation between CH_4 flux and temperature and water content in both reclamation types (Table 5). Furthermore, the positive correlation between CH_4 emissions and increased biomass is explained by plant-mediated transport and root exudation-stimulated methanogens [76]. The CH_4 fluxes in this study ranged from -3.09 to $200.32 \text{ } \mu\text{mol m}^{-2} \text{ h}^{-1}$, which is within the typical range of $2200 \pm 310 \text{ } \mu\text{mol m}^{-2} \text{ h}^{-1}$ of methane CH_4 emissions across China's coastal wetlands. Our results are similarly consistent with data from other salt marshes such as $4.8\text{--}70.5 \text{ } \mu\text{mol m}^{-2} \text{ h}^{-1}$ [29]; $97.5\text{--}313.75 \text{ } \mu\text{mol m}^{-2} \text{ h}^{-1}$ [77] for mangrove forests; 2.00 to $21.70 \text{ } \mu\text{mol m}^{-2} \text{ h}^{-1}$ [26]; $11.9\text{--}5168.6 \text{ } \mu\text{mol m}^{-2} \text{ h}^{-1}$ in Hong Kong [59]; and $5.73\text{--}201.88 \text{ } \mu\text{mol m}^{-2} \text{ h}^{-1}$ in East India [78]. By discharging exudates and producing plant litterfall, soil CH_4 emission represents a source of methanogenic substrate [29] and can be controlled by vegetation in three ways, as exemplified in [79]. The marginally significant difference observed in the regression between biomass and CH_4 emissions for the embankment restored and unrestored sections explain how plant factors such as root exudation are most likely responsible for some disparities in CH_4 flux rates across marshes. Because they promote favorable circumstances for nitrogen cycling activities, salt marshes are essential nitrogen sinks in coastal zones. Most marshes, however, are minor N_2O sinks because denitrifiers can use N_2O when nitrate is scarce [80]. Because of the increased availability of energetically more suitable nitrate due to N-loading, marshes might suddenly shift from net sinks to net sources of N_2O [81]. Such was observed in this study, as shown in Figure 6e,f. Between January and July, N_2O emissions were consistent between the restored *S. alterniflora* and *P. australis* marshes. However, an abrupt shift was observed in the *P. australis* marsh, as N_2O emission rose from $16.21 \text{ n mol m}^{-2} \text{ h}^{-1}$ in July to $534.16 \text{ n mol m}^{-2} \text{ h}^{-1}$ in August, compared to $-88.44 \text{ n mol m}^{-2} \text{ h}^{-1}$ to $80.27 \text{ n mol m}^{-2} \text{ h}^{-1}$ in the restored *S. alterniflora* marsh. These findings corroborate the evidence that *S. alterniflora* relatively lowers N_2O emission compared to *P. australis*, and thus can be regarded as a species for tidal zone stabilization [82]. The peak N_2O emission ($534.16 \text{ n mol m}^{-2} \text{ h}^{-1}$) obtained in this study exceeds the average N_2O fluxes ($373.6 \text{ n mol m}^{-2} \text{ h}^{-1}$) estimated across coastal wetlands in China [47]. The contribution of *P. australis* rhizosphere oxygenation to N_2O flux rates has also been substantiated in a freshwater wetland investigation [83]. As a result, it is reasonable to infer that embankment reclamation significantly increases N_2O emissions in a *P. australis* salt marsh as observed in this study. As a result of the increased CO_2 content in the chamber air, the CO_2 gradient between the soil and the chamber is reduced, lowering the detected fluxes. Lower fluxes could be attributed to a cooler soil temperature inside the static chamber. During the experiment, soil temperature was monitored hourly outside the chambers, which was approximately 4°C higher than the temperature within the static chambers [84]. Such diurnal variations in air temperature affects GHG estimates. The marshy environment influenced chamber positioning relative to plant tissue, which influenced the interpretation of flux data, especially in the case of CO_2 , where perhaps microbial respiration and also root and shoot respiration and photosynthesis must be properly balanced.

Owing to the anoxic and oxic conditions influenced by the above noted factors, marshes are most certainly the most significant source of soil carbon emissions in China's wetlands [74]. China's wetlands emit less CO_2 than the United States, but more than Canada, Europe, and Russia, as well as the global mean. Conversely, soil CH_4 in China's wetlands ($0.29 \text{ Mg C ha}^{-1} \text{ year}^{-1}$) is considerably less than those in America, Canada and the global average, but higher than that of Europe [74]. These variances could be explained by changes in climate and soil conditions between China and these other nations, resulting in disparities in the distribution patterns of each wetland category.

4.3. Invasion/Reclamation Context

In China, the pace of seawall construction and expansion for the primary goal of coastal land reclamation [5] and control of *Spartina alterniflora* invasion [85] has more than twice expanded in the past decades [86]. This resulted in the loss of at least 10,520 km² of habitats in the Yellow Sea [7] and triggered other ecological impacts of climate change, GHG emissions, marine pollution, etc. Our study is the first to concurrently examine the effects of a seawall embankment on GHG fluxes and stocks in *S. alterniflora* and *P. australis* dominated saltmarsh. Compared to a study that examined the patterns and drivers of greenhouse gases and flux in china's coastal wetlands [47], the average emissions of carbon dioxide (CO₂), methane (CH₄), and nitrous oxide (N₂O) were estimated to be 388.76 mg m⁻² h⁻¹, 2.20 mgm⁻²h⁻¹, and 16.44 μgm⁻²h⁻¹ respectively. Although [47] did not differentiate nor compare between reclaimed and unreclaimed wetlands, their estimates were relatively less than the averages found in the reclaimed marshes of this study (404.76 mg m⁻² h⁻¹, 3.06 mgm⁻²h⁻¹, and 23.38 μgm⁻²h⁻¹, respectively). This essentially justifies our hypothesis that seawall embankment alters GHG emissions in reclaimed wetlands, because no study assessed these effects in the area. Studies by [9,52,85] examined only the impact of seawall embankment reclamation on soil organic carbon and nitrogen pools. In all these scenarios, the seawall reclamation essentially altered soil C and N accumulation, salinity, soil moisture, total biomass, and microbial biomass, especially in the invasive plant community, as observed in this study. *S. alterniflora* invasion has been found to cause a shift in methanogen community composition and CH₄ production capability [87], increasing CH₄ emissions in China [29]. Hence, the erection of coastal embankments, which is becoming a more prevalent method of restricting the spread of *Spartina alterniflora*, provides an opportunity to reduce CH₄ emissions, as observed. However, our findings on GHG fluxes show that embankment reclamation significantly increased CO₂ and reduced CH₄ emissions in both reclamation types and increased N₂O emissions in the restored *P. australis* marsh in the warmer months. As for N₂O emissions, the potential of embankment reclamation to increase emissions in a native marsh, particularly in the warmer months, is attributable to the significance of rhizosphere oxygenation in *P. australis* on N₂O flux rates [83]. Hence, it is imperative to note that these findings may not be indicative of other parts of the world because the functions of invasive and native species are opposite in those areas; hence further investigation is needed.

5. Management Implications

In an invasive plant-dominated salt marsh, seawall construction can have negative implications such as decreased soil organic carbon and nitrogen buildup, which can lead to weak soil nitrogen nitrification/denitrification, among other effects [9,52,85]. In contrast, salt marshes, when preserved in front of seawalls, levees, and other “grey” coastal defenses, can offer protection strata that significantly mitigate floods and storms [88–90]. Paddy fields and seawalls can help to mitigate the economic damage inflicted by severe storms [91], restoring wetlands beyond the seawalls, which provides a healthier water habitat [92], whereas open dikes protect native salt marshes, resulting in almost no loss of ecosystem functions and services [6]. The eradication of *S. alterniflora* resulted in reduced CO₂, CH₄, and N₂O emissions in areas it earlier occupied, whereas CH₄ fluxes, in contrast, increased dramatically in places where the native species *P. australis* was maintained [93]. Similarly, reclamation of a *S. alterniflora* dominated salt marsh by embankment seawalls significantly reduced soil total organic carbon, total organic nitrogen, soil salinity, litter, moisture, and root biomass effects [9,52,85]. In this study, sea embankment enhanced CO₂ emissions and decreased CH₄ emissions in the *Spartina alterniflora* and *Phragmites australis* marshes, respectively. In addition, the coastal embankment wall increased N₂O emissions in the *Phragmites australis* salt marsh while decreasing emissions in the *Spartina alterniflora* marsh. Methane CH₄ and carbon dioxide CO₂ fluxes were similar in both restored and unrestored portions, whereas nitrous oxide N₂O fluxes were significantly different owing to enhanced nitrate due to N-loading. In both plants' marsh, sea embankment reclamation diminished

soil total organic C and total organic N, as well as plant biomass, soil moisture, and soil salinity. The three gases studied have their fluxes and stocks varied in both reclamation types and were linked to soil temperature, reclamation type, anoxic conditions, and living biomass. Seasonal variations in CO₂ flows were observed, as expected. As predicted in salt marshes, CH₄ production rates were moderate, but they varied substantially, indicating that CH₄ generation is highly spatially variable. The GHG stock soil measurements were obtained during the autumn period of the season, which could limit our conclusions. As such, further studies should consider the spring, summer, and winter seasons, such that spatiotemporal variations of GHG stocks in seawall reclaimed wetlands relative to alien plants invasions will yield more concrete conclusions.

Our findings corroborate the evidence that coastal reclamation by seawalls could curb *S. alterniflora* invasion while also endangering biodiversity, risks in terms of climate change mitigation, and long-term sustainability of coastal wetlands. Stakeholders in charge of ecosystem eradication initiatives and other types of restoration must therefore define their objectives and criteria for success, as evaluating the implications of coastal reclamation management options in the context of global climate change mitigation becomes more challenging in today's threatened ecosystems. At both the national and municipal levels, thorough wetland control mechanisms are required to accomplish a goal of "zero net loss" and long-term sustainability of coastal wetlands. Offsetting anthropogenic disruption and restoring damaged wetlands can enable sustained C budgets and spur global efforts to combat global warming and climate change. These findings help move us closer to the UN's goal for a steady transition to a carbon-free future and eventual GHG pollution eradication. This scientific information offers stakeholders and policymakers leverage to balance seawall reclamation and invasive plant spread in coastal wetlands. There are opportunities for further research on balancing the tradeoffs between the synergistic impacts of reclamation by invasive plant species and reclamation seawalls.

Author Contributions: Conceptualization, T.K.Y. and J.L.; methodology, T.K.Y. and D.D.; software, Z.L. and Y.W.; validation, T.K.Y., Z.L. and Y.W.; formal analysis, T.K.Y.; investigation, Z.L. and Y.W.; resources, D.D., G.L., G.R., G.W. and Y.J.; data curation, T.K.Y. and J.L.; writing—original draft preparation, T.K.Y.; writing—review and editing, T.K.Y., D.D., G.L., G.R., G.W. and Y.J.; visualization, T.K.Y., Z.L. and Y.W.; supervision, D.D.; project administration, J.L.; funding acquisition, J.L., D.D., G.L., G.R., G.W. and Y.J. All authors have read and agreed to the published version of the manuscript.

Funding: This research was funded by the National Natural Science Foundation of China (32071521, 31800429, 31760163), the Natural Science Foundation of Jiangsu Province (BK20170540), the MEL Visiting Fellowship of Xiamen University and Jiangsu Collaborative Innovation Center of Technology and Material of Water Treatment, China.

Institutional Review Board Statement: Not applicable.

Informed Consent Statement: Not applicable.

Data Availability Statement: Not applicable.

Conflicts of Interest: The authors declare no conflict of interest.

References

1. Yuguda, T.K.; Li, Y.; Luka, B.S.; Dzarma, G.W. Incorporating Reservoir Greenhouse Gas Emissions into Carbon Footprint of Sugar Produced from Irrigated Sugarcane in Northeastern Nigeria. *Sustainability* **2020**, *12*, 10380. [\[CrossRef\]](#)
2. Davidson, N.C. How much wetland has the world lost? Long-term and recent trends in global wetland area. *Mar. Freshw. Res.* **2014**, *65*, 934–941. [\[CrossRef\]](#)
3. Dafforn, K.A. Eco-engineering and management strategies for marine infrastructure to reduce establishment and dispersal of non-indigenous species. *Manag. Biol. Invasions* **2017**, *8*, 153–161. [\[CrossRef\]](#)
4. Sun, X.; Li, Y.; Zhu, X.; Cao, K.; Feng, L. Integrative assessment and management implications on ecosystem services loss of coastal wetlands due to reclamation. *J. Clean. Prod.* **2017**, *163*, S101–S112. [\[CrossRef\]](#)
5. Ma, Z.; Melville, D.S.; Liu, J.; Chen, Y.; Yang, H.; Ren, W.; Zhang, Z.; Piersma, T.; Li, B. Rethinking China's new great wall. *Science* **2014**, *346*, 912–914. [\[CrossRef\]](#)

6. Wu, W.; Yang, Z.; Tian, B.; Huang, Y.; Zhou, Y.; Zhang, T. Impacts of coastal reclamation on wetlands: Loss, resilience, and sustainable management. *Estuar. Coast. Shelf Sci.* **2018**, *210*, 153–161. [\[CrossRef\]](#)
7. Choi, C.Y.; Jackson, M.V.; Gallo-Cajiao, E.; Murray, N.J.; Clemens, R.S.; Gan, X.; Fuller, R.A. Biodiversity and China's new Great Wall. *Divers. Distrib.* **2018**, *24*, 137–143. [\[CrossRef\]](#)
8. Bulleri, F.; Chapman, M.G. The introduction of coastal infrastructure as a driver of change in marine environments. *J. Appl. Ecol.* **2010**, *47*, 26–35. [\[CrossRef\]](#)
9. Yang, W.; Li, N.; Leng, X.; Qiao, Y.; Cheng, X.; An, S. The impact of sea embankment reclamation on soil organic carbon and nitrogen pools in invasive *Spartina alterniflora* and native *Suaeda salsa* salt marshes in eastern China. *Ecol. Eng.* **2016**, *97*, 582–592. [\[CrossRef\]](#)
10. Olefeldt, D.; Euskirchen, E.S.; Harden, J.; Kane, E.; McGuire, A.D.; Waldrop, M.P.; Turetsky, M.R. A decade of boreal rich fen greenhouse gas fluxes in response to natural and experimental water table variability. *Glob. Chang. Biol.* **2017**, *23*, 2428–2440. [\[CrossRef\]](#) [\[PubMed\]](#)
11. Ma, T.; Li, X.; Bai, J.; Ding, S.; Zhou, F.; Cui, B. Four decades' dynamics of coastal blue carbon storage driven by land use/land cover transformation under natural and anthropogenic processes in the Yellow River Delta, China. *Sci. Total Environ.* **2019**, *655*, 741–750. [\[CrossRef\]](#)
12. Misra, A.; Balaji, R. Decadal changes in the land use/land cover and shoreline along the coastal districts of southern Gujarat, India. *Environ. Monit. Assess.* **2015**, *187*. [\[CrossRef\]](#) [\[PubMed\]](#)
13. Misra, A.; Balaji, R. A Study on the Shoreline Changes and LAND-use/ Land-cover along the South Gujarat Coastline. *Procedia Eng.* **2015**, *116*, 381–389. [\[CrossRef\]](#)
14. Kumar Pramanik, M.; Pramanik, M.K. Impacts of predicted sea level rise on land use/land cover categories of the adjacent coastal areas of Mumbai megacity, India. *Environ. Dev. Sustain.* **2017**, *19*, 1343–1366. [\[CrossRef\]](#)
15. Riitters, K.; Potter, K.; Iannone, B.V., III; Oswalt, C.; Fei, S.; Guo, Q. Landscape correlates of forest plant invasions: A high-resolution analysis across the eastern United States. *Divers. Distrib.* **2018**, *24*, 274–284. [\[CrossRef\]](#)
16. Gibson, L.; Münch, Z.; Palmer, A.; Mantel, S. Future land cover change scenarios in South African grasslands – implications of altered biophysical drivers on land management. *Heliyon* **2018**, *4*, e00693. [\[CrossRef\]](#)
17. González-Moreno, P.; Pino, J.; Cózar, A.; García-De-Lomas, J.; Vilà, M. The effects of landscape history and time-lags on plant invasion in Mediterranean coastal habitats. *Biol. Invasions* **2017**, *19*, 549–561. [\[CrossRef\]](#)
18. Basnou, C.; Iguzquiza, J.; Pino, J. Examining the role of landscape structure and dynamics in alien plant invasion from urban Mediterranean coastal habitats. *Landsc. Urban Plan.* **2015**, *136*, 156–164. [\[CrossRef\]](#)
19. Nobis, A.; Żmihorski, M.; Kotowska, D. Linking the diversity of native flora to land cover heterogeneity and plant invasions in a river valley. *Biol. Conserv.* **2016**, *203*, 17–24. [\[CrossRef\]](#)
20. Seebens, H.; Blackburn, T.M.; Dyer, E.E.; Genovesi, P.; Hulme, P.E.; Jeschke, J.M.; Pagad, S.; Pyšek, P.; Winter, M.; Arianoutsou, M.; et al. No saturation in the accumulation of alien species worldwide. *Nat. Commun.* **2017**, *8*, 14435. [\[CrossRef\]](#)
21. Fiselier, J.; Vreman, B.-J.; Dekker, S.; Thorborg, H. Ecosystem Based Carbon Footprinting of Marine Engineering Projects. In *Proceedings of the Coastal Management*; ICE Publishing: London, UK, 2016; pp. 355–364.
22. Wang, Y.; Wang, Z.-L.; Feng, X.; Guo, C.; Chen, Q. Long-Term Effect of Agricultural Reclamation on Soil Chemical Properties of a Coastal Saline Marsh in Bohai Rim, Northern China. *PLoS ONE* **2014**, *9*, e93727. [\[CrossRef\]](#)
23. Bu, N.S.; Qu, J.F.; Li, G.; Zhao, B.; Zhang, R.J.; Fang, C.M. Reclamation of coastal salt marshes promoted carbon loss from previously-sequestered soil carbon pool. *Ecol. Eng.* **2015**, *81*, 335–339. [\[CrossRef\]](#)
24. Emery, H.E.; Fulweiler, R.W. *Spartina alterniflora* and invasive *Phragmites australis* stands have similar greenhouse gas emissions in a New England marsh. *Aquat. Bot.* **2014**, *116*, 83–92. [\[CrossRef\]](#)
25. Duman, T.; Schäfer, K.V.R. Partitioning net ecosystem carbon exchange of native and invasive plant communities by vegetation cover in an urban tidal wetland in the New Jersey Meadowlands (USA). *Ecol. Eng.* **2018**, *114*, 16–24. [\[CrossRef\]](#)
26. Chen, Y.; Chen, G.; Ye, Y. Coastal vegetation invasion increases greenhouse gas emission from wetland soils but also increases soil carbon accumulation. *Sci. Total Environ.* **2015**, *526*, 19–28. [\[CrossRef\]](#)
27. Schäfer, K.V.R.; Duman, T.; Tomasicchio, K.; Tripathi, R.; Sturtevant, C. Carbon dioxide fluxes of temperate urban wetlands with different restoration history. *Agric. For. Meteorol.* **2019**, *275*, 223–232. [\[CrossRef\]](#)
28. Meng, W.; Feagin, R.A.; Hu, B.; He, M.; Li, H. The spatial distribution of blue carbon in the coastal wetlands of China. *Estuar. Coast. Shelf Sci.* **2019**, *222*, 13–20. [\[CrossRef\]](#)
29. Tong, C.; Wang, W.Q.; Huang, J.F.; Gauci, V.; Zhang, L.H.; Zeng, C.S. Invasive alien plants increase CH₄ emissions from a subtropical tidal estuarine wetland. *Biogeochemistry* **2012**, *111*, 677–693. [\[CrossRef\]](#)
30. Abdul-Aziz, O.I.; Ishtiaq, K.S.; Tang, J.; Moseman-Valtierra, S.; Kroeger, K.D.; Gonneea, M.E.; Mora, J.; Morkeski, K. Environmental Controls, Emergent Scaling, and Predictions of Greenhouse Gas (GHG) Fluxes in Coastal Salt Marshes. *J. Geophys. Res. Biogeosci.* **2018**, *123*, 2234–2256. [\[CrossRef\]](#)
31. Cabezas, A.; Mitsch, W.J.; MacDonnell, C.; Zhang, L.; Bydalek, F.; Lasso, A. Methane emissions from mangrove soils in hydrologically disturbed and reference mangrove tidal creeks in southwest Florida. *Ecol. Eng.* **2018**, *114*, 57–65. [\[CrossRef\]](#)
32. Yin, S.; An, S.; Deng, Q.; Zhang, J.; Ji, H.; Cheng, X. *Spartina alterniflora* invasions impact CH₄ and N₂O fluxes from a salt marsh in eastern China. *Ecol. Eng.* **2015**, *81*, 192–199. [\[CrossRef\]](#)

33. Zhang, Y.; Wang, L.; Xie, X.; Huang, L.; Wu, Y. Effects of invasion of *Spartina alterniflora* and exogenous N deposition on N₂O emissions in a coastal salt marsh. *Ecol. Eng.* **2013**, *58*, 77–83. [\[CrossRef\]](#)
34. Rey-Sanchez, A.C.; Morin, T.H.; Stefanik, K.C.; Wrighton, K.; Bohrer, G. Determining total emissions and environmental drivers of methane flux in a Lake Erie estuarine marsh. *Ecol. Eng.* **2018**, *114*, 7–15. [\[CrossRef\]](#)
35. Xu, C.; Wong, V.N.L.; Reef, R.E. Effect of inundation on greenhouse gas emissions from temperate coastal wetland soils with different vegetation types in southern Australia. *Sci. Total Environ.* **2021**, *763*, 142949. [\[CrossRef\]](#) [\[PubMed\]](#)
36. Lu, W.; Liu, C.; Zhang, Y.; Yu, C.; Cong, P.; Ma, J.; Xiao, J. Carbon fluxes and stocks in a carbonate-rich chenier plain. *Agric. For. Meteorol.* **2019**, *275*, 159–169. [\[CrossRef\]](#)
37. Bastviken, D.; Tranvik, L.J.; Downing, J.A.; Crill, P.M.; Enrich-Prast, A. Freshwater methane emissions offset the continental carbon sink. *Science* **2011**, *331*, 50. [\[CrossRef\]](#)
38. Yang, W.; Zhao, H.; Leng, X.; Cheng, X.; An, S. Soil organic carbon and nitrogen dynamics following *Spartina alterniflora* invasion in a coastal wetland of eastern China. *Catena* **2017**, *156*, 281–289. [\[CrossRef\]](#)
39. Zhang, Y.; Ding, W.; Luo, J.; Donnison, A. Changes in soil organic carbon dynamics in an Eastern Chinese coastal wetland following invasion by a C4 plant *Spartina alterniflora*. *Soil Biol. Biochem.* **2010**, *42*, 1712–1720. [\[CrossRef\]](#)
40. Zhang, G.; Bai, J.; Zhao, Q.; Jia, J.; Wang, X.; Wang, W.; Wang, X. Soil carbon storage and carbon sources under different *Spartina alterniflora* invasion periods in a salt marsh ecosystem. *Catena* **2021**, *196*. [\[CrossRef\]](#)
41. Huang, Y.; Chen, Z.; Tian, B.; Zhou, C.; Wang, J.; Ge, Z.; Tang, J. Tidal effects on ecosystem CO₂ exchange in a *Phragmites* salt marsh of an intertidal shoal. *Agric. For. Meteorol.* **2020**, *292*–293. [\[CrossRef\]](#)
42. Yang, W.; Zhao, H.; Chen, X.; Yin, S.; Cheng, X.; An, S. Consequences of short-term C4 plant *Spartina alterniflora* invasions for soil organic carbon dynamics in a coastal wetland of Eastern China. *Ecol. Eng.* **2013**, *61*, 50–57. [\[CrossRef\]](#)
43. DeLaune, R.D.; White, J.R.; Elsey-Quirk, T.; Roberts, H.H.; Wang, D.Q. Differences in long-term vs short-term carbon and nitrogen sequestration in a coastal river delta wetland: Implications for global budgets. *Org. Geochem.* **2018**, *123*, 67–73. [\[CrossRef\]](#)
44. Villa, J.A.; Bernal, B. Carbon sequestration in wetlands, from science to practice: An overview of the biogeochemical process, measurement methods, and policy framework. *Ecol. Eng.* **2018**, *114*, 115–128. [\[CrossRef\]](#)
45. Falkowski, P.; Scholes, R.J.; Boyle, E.; Canadell, J.; Canfield, D.; Elser, J.; Gruber, N.; Hibbard, K.; Höglberg, P.; Linder, S.; et al. The Global Carbon Cycle: A Test of Our Knowledge of Earth as a System. *Science* **2000**, *290*, 291–296. [\[CrossRef\]](#)
46. Yu, G.-R.; Zhu, X.-J.; Fu, Y.-L.; He, H.-L.; Wang, Q.-F.; Wen, X.-F.; Li, X.-R.; Zhang, L.-M.; Zhang, L.; Su, W.; et al. Spatial patterns and climate drivers of carbon fluxes in terrestrial ecosystems of China. *Glob. Chang. Biol.* **2013**, *19*, 798–810. [\[CrossRef\]](#)
47. Hu, M.; Sardans, J.; Yang, X.; Peñuelas, J.; Tong, C. Patterns and environmental drivers of greenhouse gas fluxes in the coastal wetlands of China: A systematic review and synthesis. *Environ. Res.* **2020**, *186*, 109576. [\[CrossRef\]](#) [\[PubMed\]](#)
48. Lawrence, B.A.; Lishawa, S.C.; Hurst, N.; Castillo, B.T.; Tuchman, N.C. Wetland invasion by *Typha × glauca* increases soil methane emissions. *Aquat. Bot.* **2017**, *137*, 80–87. [\[CrossRef\]](#)
49. Al-Haj, A.N.; Fulweiler, R.W. A synthesis of methane emissions from shallow vegetated coastal ecosystems. *Glob. Chang. Biol.* **2020**, *26*, 2988–3005. [\[CrossRef\]](#) [\[PubMed\]](#)
50. Gao, G.F.; Li, P.F.; Zhong, J.X.; Shen, Z.J.; Chen, J.; Li, Y.T.; Isabwe, A.; Zhu, X.Y.; Ding, Q.S.; Zhang, S.; et al. *Spartina alterniflora* invasion alters soil bacterial communities and enhances soil N₂O emissions by stimulating soil denitrification in mangrove wetland. *Sci. Total Environ.* **2019**, *653*, 231–240. [\[CrossRef\]](#)
51. Li, J.; Pu, L.; Zhu, M.; Zhang, J.; Li, P.; Dai, X.; Xu, Y.; Liu, L. Evolution of soil properties following reclamation in coastal areas: A review. *Geoderma* **2014**, *226*–227, 130–139. [\[CrossRef\]](#)
52. Zhou, S.; Bi, X. Seawall effects in a coastal wetland landscape: Spatial changes in soil carbon and nitrogen pools. *J. Coast. Conserv.* **2020**, *24*, 1–9. [\[CrossRef\]](#)
53. Yang, W.; Yan, Y.; Jiang, F.; Leng, X.; Cheng, X.; An, S. Response of the soil microbial community composition and biomass to a short-term *Spartina alterniflora* invasion in a coastal wetland of eastern China. *Plant Soil* **2016**, *408*, 443–456. [\[CrossRef\]](#)
54. Hirota, M.; Senga, Y.; Seike, Y.; Nohara, S.; Kunii, H. Fluxes of carbon dioxide, methane and nitrous oxide in two contrastive fringing zones of coastal lagoon, Lake Nakaumi, Japan. *Chemosphere* **2007**, *68*, 597–603. [\[CrossRef\]](#)
55. Tan, L.; Ge, Z.; Zhou, X.; Li, S.; Li, X.; Tang, J. Conversion of coastal wetlands, riparian wetlands, and peatlands increases greenhouse gas emissions: A global meta-analysis. *Glob. Chang. Biol.* **2020**, *26*, 1638–1653. [\[CrossRef\]](#)
56. Xie, G.; Wang, B.; Zhao, K.; Li, S.; Zhou, L. Dynamic Changes of Animal Community Composition and Distribution by *Spartina* Invasion in Yancheng Beach Wetland, China. *CLEAN Soil Air Water* **2015**, *43*, 1409–1418. [\[CrossRef\]](#)
57. Xie, G.; He, F.; Xie, T.; Huang, C.; Tang, B. Influence of *Spartina* invasion to Jiangsu Province's beach wetland animal community. *Dongbei Nongye Daxue Xuebao* **2011**, *42*, 68–76.
58. Chung, C.H.; Zhuo, R.Z.; Xu, G.W. Creation of *Spartina* plantations for reclaiming Dongtai, China, tidal flats and offshore sands. *Ecol. Eng.* **2004**, *23*, 135–150. [\[CrossRef\]](#)
59. Chen, G.C.; Tam, N.F.Y.; Ye, Y. Summer fluxes of atmospheric greenhouse gases N₂O, CH₄ and CO₂ from mangrove soil in South China. *Sci. Total Environ.* **2010**, *408*, 2761–2767. [\[CrossRef\]](#) [\[PubMed\]](#)
60. Chen, G.C.; Tam, N.F.Y.; Wong, Y.S.; Ye, Y. Effect of wastewater discharge on greenhouse gas fluxes from mangrove soils. *Atmos. Environ.* **2011**, *45*, 1110–1115. [\[CrossRef\]](#)
61. Chen, G.; Chen, B.; Yu, D.; Ye, Y.; Tam, N.; Chen, S. Soil greenhouse gases emissions reduce the benefit of mangrove plant to mitigating atmospheric warming effect. *Biogeosci. Discuss.* **2016**, 1–22. [\[CrossRef\]](#)

62. IPCC. *Climate Change 2014: Impacts, Adaptation and Vulnerability*; IPCC: Geneva, Switzerland, 2014.
63. Campbell, J.E.; Lacey, E.A.; Decker, R.A.; Crooks, S.; Fourqurean, J.W. Carbon Storage in Seagrass Beds of Abu Dhabi, United Arab Emirates. *Estuaries Coasts* **2015**, *38*, 242–251. [\[CrossRef\]](#)
64. Smith, S.V. *Parsing the Oceanic Calcium Carbonate Cycle: A Net Atmospheric Carbon Dioxide Source or a Sink?* Association for the Sciences of Limnology and Oceanography: Waco, TX, USA, 2013; ISBN 9780984559121.
65. Mazarrasa, I.; Marbà, N.; Lovelock, C.; Serrano, O.; Lavery, P.S.; Fourqurean, J.W.; Kennedy, H.; Mateo, M.A.; Krause-Jensen, D.; Steven, A.D.L.; et al. Seagrass meadows as a globally significant carbonate reservoir. *Biogeosciences* **2015**, *12*, 4993–5003. [\[CrossRef\]](#)
66. Bai, J.; Xiao, R.; Zhang, K.; Gao, H.; Cui, B.; Liu, X. Soil organic carbon as affected by land use in young and old reclaimed regions of a coastal estuary wetland, China. *Soil Use Manag.* **2013**, *29*, 57–64. [\[CrossRef\]](#)
67. Wang, H.; Wang, R.; Yu, Y.; Mitchell, M.J.; Zhang, L. Soil organic carbon of degraded wetlands treated with freshwater in the Yellow River Delta, China. *J. Environ. Manag.* **2011**, *92*, 2628–2633. [\[CrossRef\]](#)
68. Zhong, C.; Wang, J.; Limnology, P.Q.-T.O. Relationship of salt marsh plant distribution and soil physical and chemical characteristic in coastal salt marsh plant of north Jiangsu Province. *Trans. Oceanol. Limnol.* **2011**, *4*, 021.
69. Yang, W.; An, S.; Zhao, H.; Xu, L.; Qiao, Y.; Cheng, X. Impacts of *Spartina alterniflora* invasion on soil organic carbon and nitrogen pools sizes, stability, and turnover in a coastal salt marsh of eastern China. *Ecol. Eng.* **2016**, *86*, 174–182. [\[CrossRef\]](#)
70. Meng, W.; Feagin, R.A.; Innocenti, R.A.; Hu, B.; He, M.; Li, H. Invasion and ecological effects of exotic smooth cordgrass *Spartina alterniflora* in China. *Ecol. Eng.* **2020**, *143*, 105670. [\[CrossRef\]](#)
71. Duarte, C.M.; Middelburg, J.J.; Caraco, N. Major role of marine vegetation on the oceanic carbon cycle. *Biogeosciences* **2005**, *2*, 1–8. [\[CrossRef\]](#)
72. McLeod, E.; Chmura, G.L.; Bouillon, S.; Salm, R.; Björk, M.; Duarte, C.M.; Lovelock, C.E.; Schlesinger, W.H.; Silliman, B.R. A blueprint for blue carbon: Toward an improved understanding of the role of vegetated coastal habitats in sequestering CO₂. *Front. Ecol. Environ.* **2011**, *9*, 552–560. [\[CrossRef\]](#)
73. Whiting, G.J.; Chanton, J.P. Greenhouse carbon balance of wetlands: Methane emission versus carbon sequestration. *Tellus Ser. B Chem. Phys. Meteorol.* **2001**, *53*, 521–528. [\[CrossRef\]](#)
74. Xiao, D.; Deng, L.; Kim, D.G.; Huang, C.; Tian, K. Carbon budgets of wetland ecosystems in China. *Glob. Chang. Biol.* **2019**, *25*, 2061–2076. [\[CrossRef\]](#)
75. Laanbroek, H.J. Methane emission from natural wetlands: Interplay between emergent macrophytes and soil microbial processes. A mini-review. *Ann. Bot.* **2010**, *105*, 141–153. [\[CrossRef\]](#) [\[PubMed\]](#)
76. Cheng, X.; Peng, R.; Chen, J.; Luo, Y.; Zhang, Q.; An, S.; Chen, J.; Li, B. CH₄ and N₂O emissions from *Spartina alterniflora* and *Phragmites australis* in experimental mesocosms. *Chemosphere* **2007**, *68*, 420–427. [\[CrossRef\]](#) [\[PubMed\]](#)
77. Wang, Z.P.; Han, X.G. Diurnal variation in methane emissions in relation to plants and environmental variables in the Inner Mongolia marshes. *Atmos. Environ.* **2005**, *39*, 6295–6305. [\[CrossRef\]](#)
78. Chauhan, R.; Ramanathan, A.L.; Adhya, T.K. Assessment of methane and nitrous oxide flux from mangroves along Eastern coast of India. *Geofluids* **2008**, *8*, 321–332. [\[CrossRef\]](#)
79. Van der Nat, F.-J.; Middelburg, J.J. Methane emission from tidal freshwater marshes. *Biogeochemistry* **2000**, *49*, 103–121. [\[CrossRef\]](#)
80. Martin, R.M.; Moseman-Valtierra, S. Greenhouse Gas Fluxes Vary Between *Phragmites Australis* and Native Vegetation Zones in Coastal Wetlands Along a Salinity Gradient. *Wetlands* **2015**, *35*, 1021–1031. [\[CrossRef\]](#)
81. Moseman-Valtierra, S.; Gonzalez, R.; Kroeger, K.D.; Tang, J.; Chao, W.C.; Crusius, J.; Bratton, J.; Green, A.; Shelton, J. Short-term nitrogen additions can shift a coastal wetland from a sink to a source of N₂O. *Atmos. Environ.* **2011**, *45*, 4390–4397. [\[CrossRef\]](#)
82. Yang, B.; Li, X.; Lin, S.; Xie, Z.; Yuan, Y.; Espenberg, M.; Pärn, J.; Mander, Ü. Invasive *Spartina alterniflora* can mitigate N₂O emission in coastal salt marshes. *Ecol. Eng.* **2020**, *147*. [\[CrossRef\]](#)
83. Yang, Z.; Zhao, Y.; Xia, X. Nitrous oxide emissions from *Phragmites australis*-dominated zones in a shallow lake. *Environ. Pollut.* **2012**, *166*, 116–124. [\[CrossRef\]](#)
84. Rochette, P.; Gregorich, E.G.; Desjardins, R.L. Comparison of static and dynamic closed chambers for measurement of soil respiration under field conditions. *Can. J. Soil Sci.* **1992**, *72*, 605–609. [\[CrossRef\]](#)
85. Yang, W.; Qiao, Y.; Li, N.; Zhao, H.; Yang, R.; Leng, X.; Cheng, X.; An, S. Seawall construction alters soil carbon and nitrogen dynamics and soil microbial biomass in an invasive *Spartina alterniflora* salt marsh in eastern China. *Appl. Soil Ecol.* **2017**, *110*, 1–11. [\[CrossRef\]](#)
86. Zhang, X.; Yan, C.; Xu, P.; Dai, Y.; Yan, W.; Ding, X.; Zhu, C.; Mei, D. Historical evolution of tidal flat reclamation in the Jiangsu coastal areas. *Dili Xuebao Acta Geogr. Sin.* **2013**, *68*, 1549–1558. [\[CrossRef\]](#)
87. Yuan, J.; Ding, W.; Liu, D.; Xiang, J.; Lin, Y. Methane production potential and methanogenic archaea community dynamics along the *Spartina alterniflora* invasion chronosequence in a coastal salt marsh. *Appl. Microbiol. Biotechnol.* **2013**, *98*, 1817–1829. [\[CrossRef\]](#) [\[PubMed\]](#)
88. Ouyang, X.; Lee, S.Y.; Connolly, R.M.; Kainz, M.J. Spatially-explicit valuation of coastal wetlands for cyclone mitigation in Australia and China. *Sci. Rep.* **2018**, *8*, 3035. [\[CrossRef\]](#)
89. Liu, X.; Wang, Y.; Costanza, R.; Kubiszewski, I.; Xu, N.; Yuan, M.; Geng, R. The value of China's coastal wetlands and seawalls for storm protection. *Ecosyst. Serv.* **2019**, *36*, 100905. [\[CrossRef\]](#)
90. Zhu, Z.; Vuik, V.; Visser, P.J.; Soens, T.; van Wesenbeeck, B.; van de Koppel, J.; Jonkman, S.N.; Temmerman, S.; Bouma, T.J. Historic storms and the hidden value of coastal wetlands for nature-based flood defence. *Nat. Sustain.* **2020**, *3*, 853–862. [\[CrossRef\]](#)

-
91. Geng, R.; Liu, X.; Lv, X.; Gao, Z.; Xu, N. Comparing cost-effectiveness of paddy fields and seawalls for coastal protection to reduce economic damage of typhoons in China. *Ecosyst. Serv.* **2021**, *47*, 101232. [[CrossRef](#)]
 92. Chen, X.; Huang, Y.; Yang, H.; Pan, L.; Perry, D.C.; Xu, P.; Tang, J.; You, W.; He, X.; Wen, Q. Restoring wetlands outside of the seawalls and to provide clean water habitat. *Sci. Total Environ.* **2020**, *721*, 137788. [[CrossRef](#)]
 93. Sheng, Q.; Zhao, B.; Huang, M.; Wang, L.; Quan, Z.; Fang, C.; Li, B.; Wu, J. Greenhouse gas emissions following an invasive plant eradication program. *Ecol. Eng.* **2014**, *73*, 229–237. [[CrossRef](#)]